ITMO UNIVERSITY
metalab.ifmo.ru

Перовскитные светоизлучающие и лазирующие нано- и микроструктуры

Сергей Макаров

рук. Лаборатории Гибридной Нанофотоники и Оптоэлектроники ("PeroLab")

Университет ИТМО

Санкт-Петербург, Россия

ФТИ, 15.04.2019

Outline

- ✓ Introduction to halide perovskites
- ✓ Reversibly tunable perovskite nanoantennas
- ✓ Extremely fast method of nanowire lasers synthesis
- ✓ Large-scale laser printing of perovskite microlasers
- ✓ All-dielectric nanolasers…

I. Introduction to perovskites

Perovskites: XIX century

Discovered perovskite…

sponsored…

Gustav Rose (1839)

Lev Perovski

$CaTiO_3$

first perovskite (**$CaTiO_3$**) was discovered by **Gustav Rose** in 1839 in Ural mountains of Russia and named after Russian minister and mineralogist **Lev Perovski.**

Perovskites: XX century

Described perovskite structure

Victor Goldschmidt (1938)

Halide perovskites

- J. Phys. C12 (1979) 5933.
- J. Phys. Soc. Jpn. 47 (1979) 232.
- Acta Cryst. A36 (1980) 7.

First organic-inorganic halide perovskites

David Mitzi @ IBM (around 1995)

ABX_3

$CaTiO_3$

$BaTiO_3$

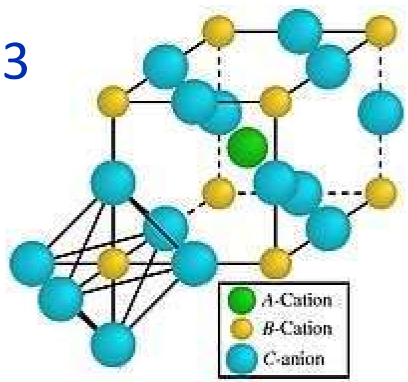

$CsPbI_3$

$CsPbBr_3$

$CsPbCl_3$

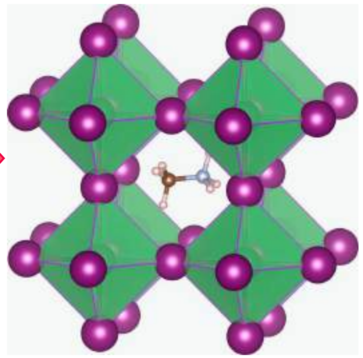

$MAPbI_3$

$MAPbBr_3$

$MAPbCl_3$

$MA = CH_3NH_3$

ITMO UNIVERSITY
metalab.ifmo.ru

Revolution in photovoltaics

Thin film photovoltaics 23.3% (2018)

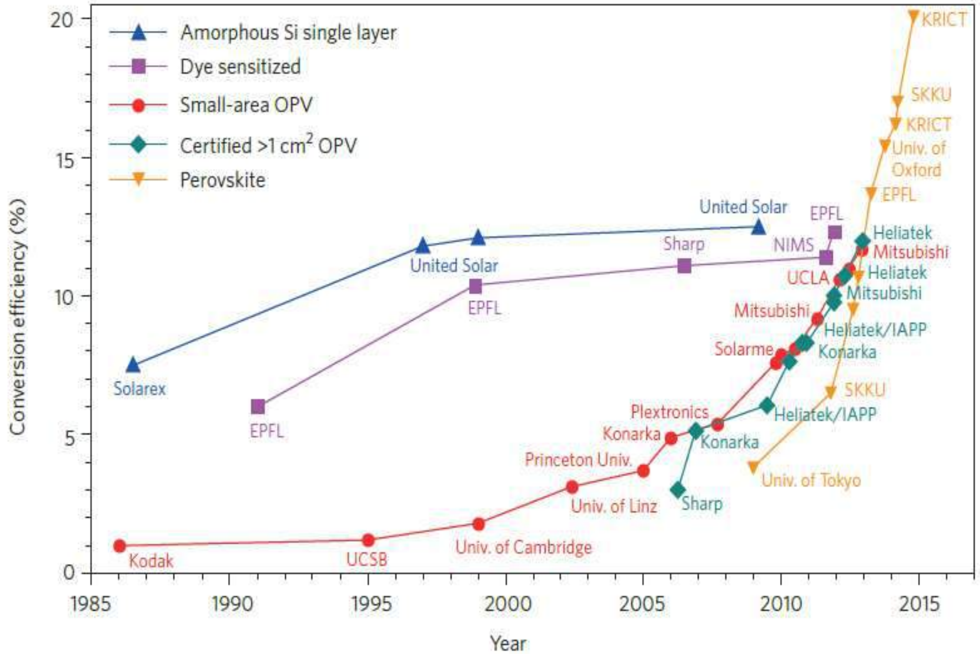

wet chemistry processing

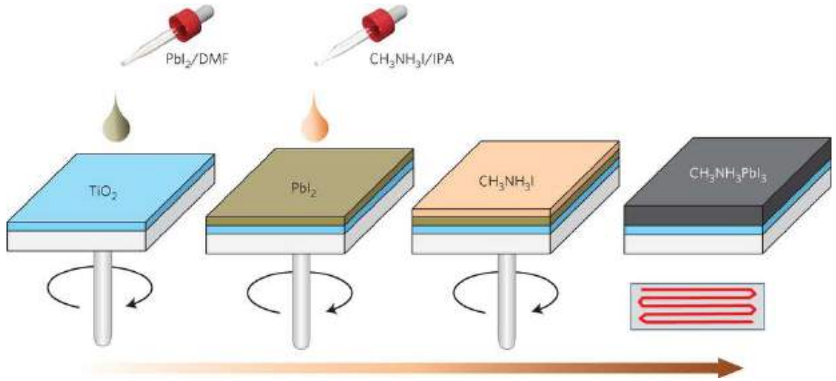

- *Low cost process*
- *Flexible substrate*
- *Tandem Perovskite-Silicon application*

nature COMMUNICATIONS

ARTICLE

Received 19 Aug 2016 | Accepted 20 Apr 2017 | Published 1 Jun 2017 DOI: 10.1038/ncomms15684 OPEN

One-Year stable perovskite solar cells by 2D/3D interface engineering

G. Grancini[1], C. Roldán-Carmona[1], I. Zimmermann[1], E. Mosconi[2,3], X. Lee[4], D. Martineau[5], S. Narbey[5], F. Oswald[5], F. De Angelis[2,3], M. Graetzel[4] & Mohammad Khaja Nazeeruddin[1]

Light-emitting properties and PeroLEDs

Bulk perovskites and quantum dots

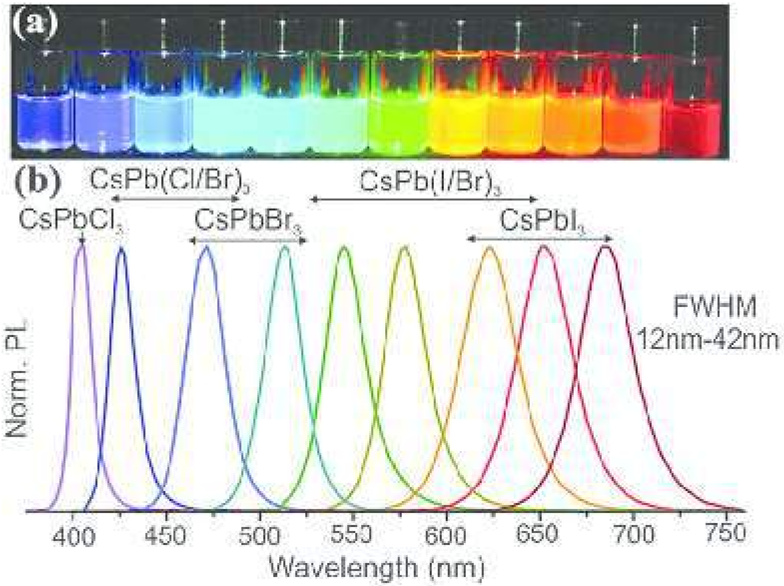

- High PL quantum yield: 50-90%
- Tuning in entire visible range
- Narrow luminescence spectra
- Flexible

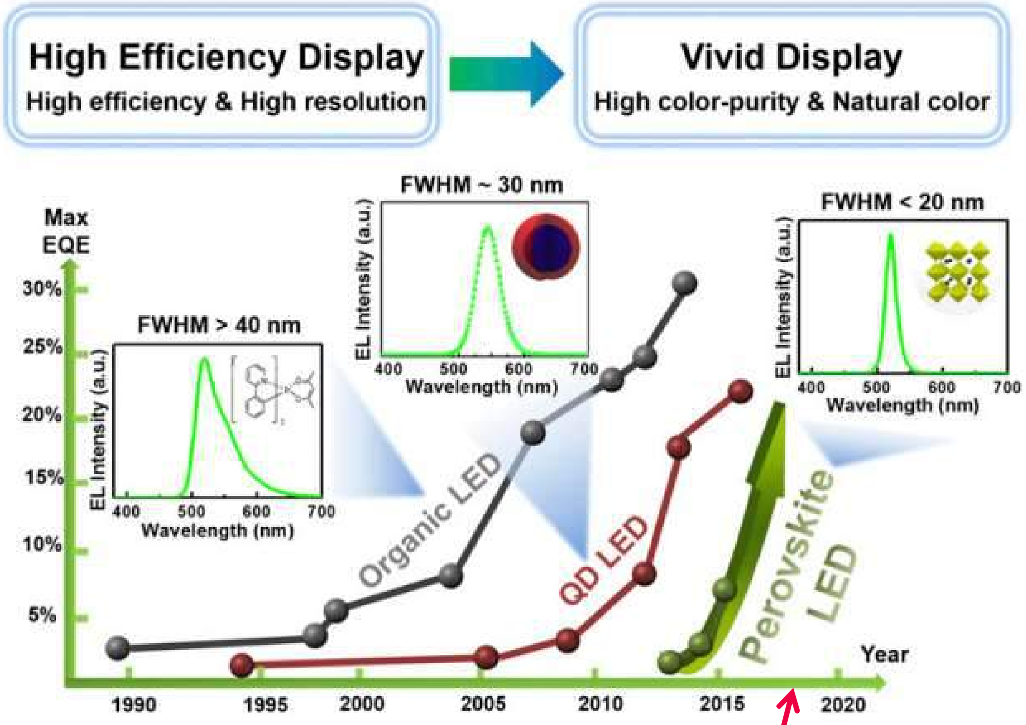

More than 20%
Nature 562 (7726), 245 (2018)

Perovskite lasers

continuos wave excitation

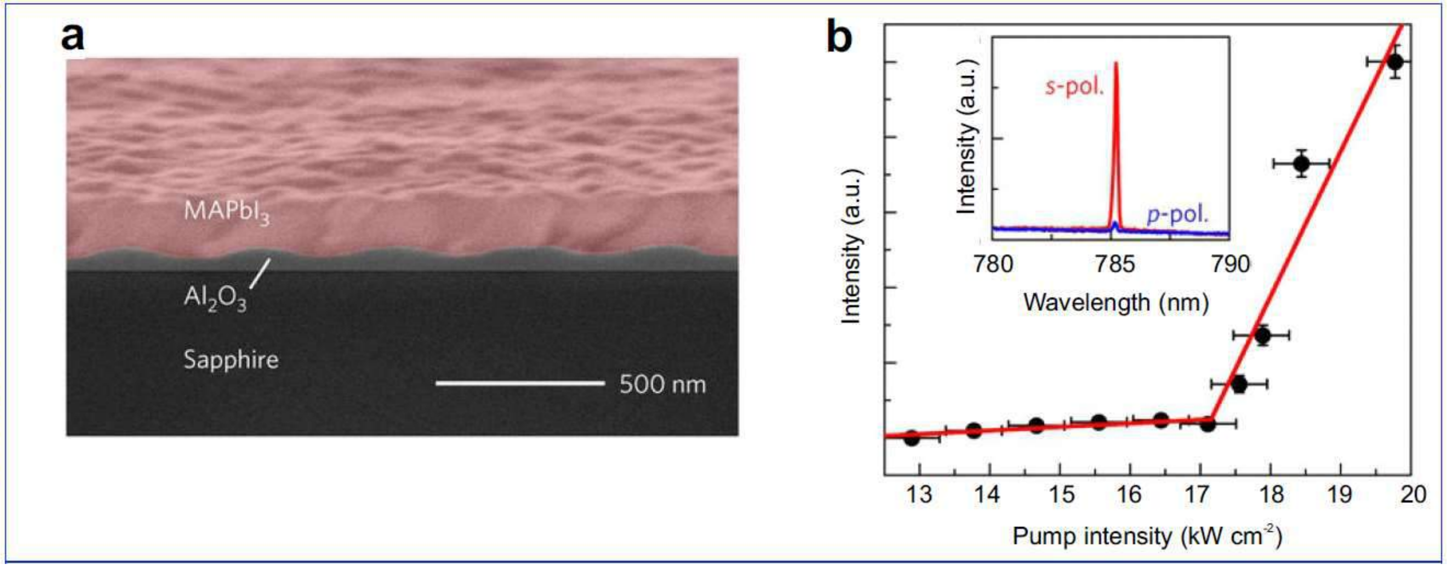

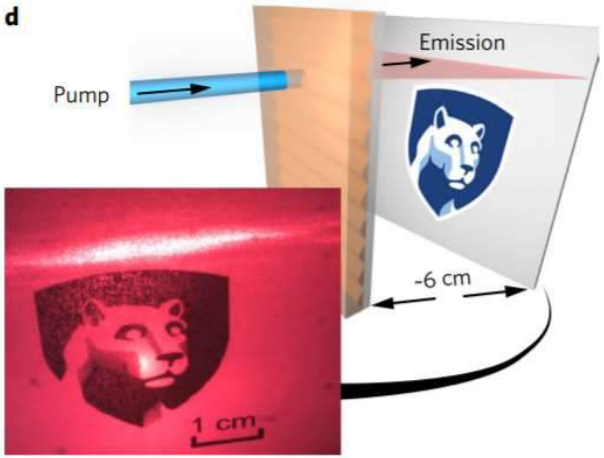

- High gain, low-threshold
- Tuning in entire visible range
- Flexible
- Electrical pump is possible

Nature Photonics 11, 784 (2017)

Basic properties of halide perovskites

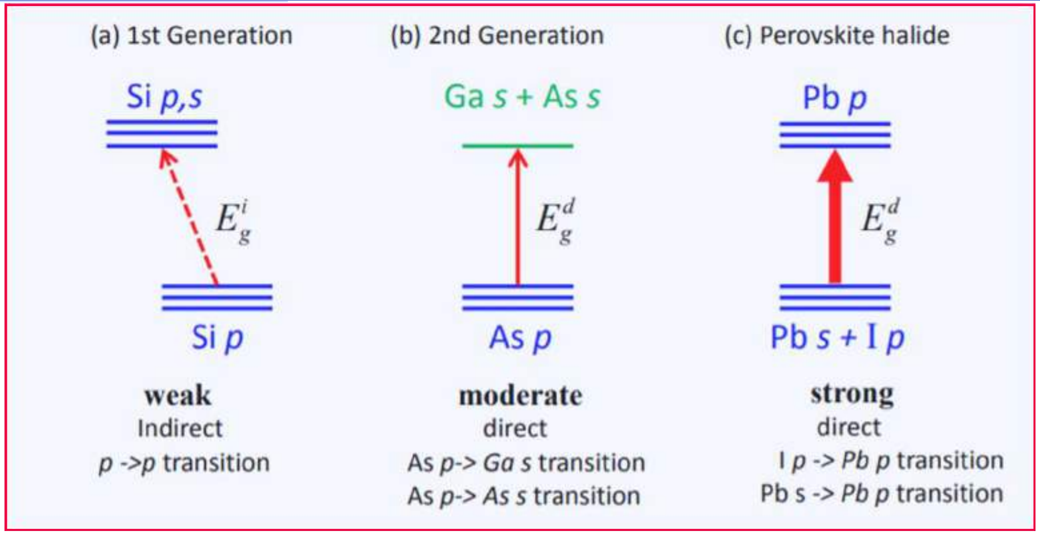

High light absorption

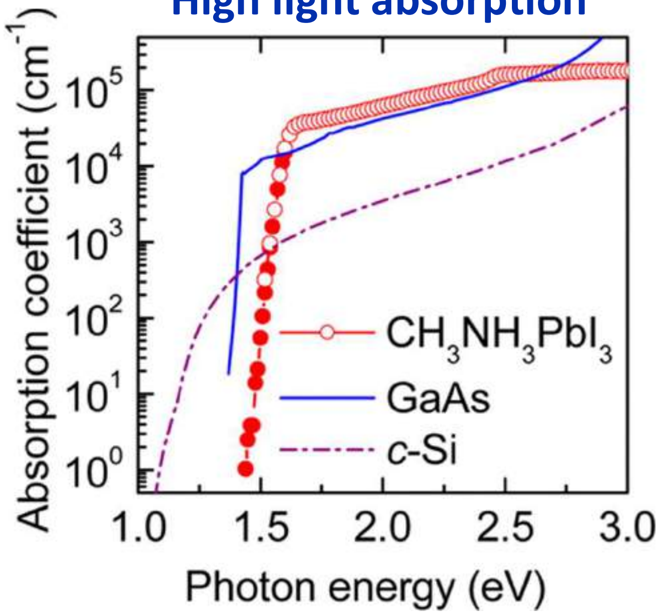

High quantum yield

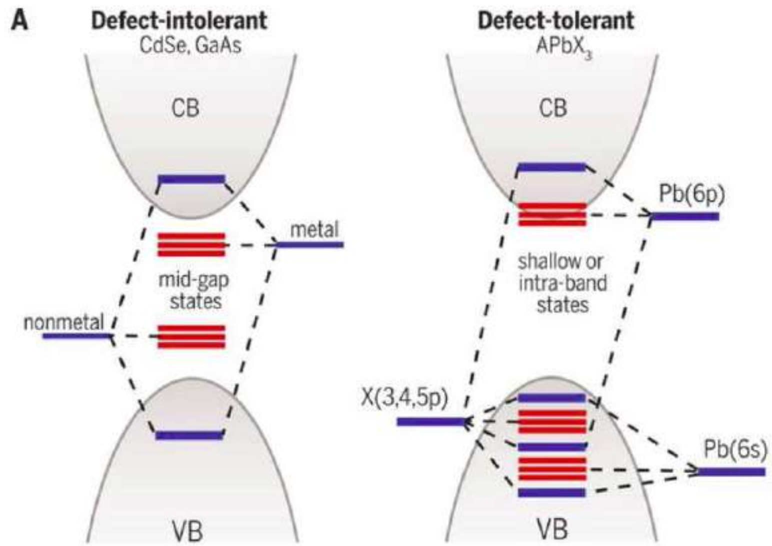

Wan-Jian Yin et al. Journ.Mat.Chem. A (2014)

Basic materials of all-dielectric nanophotonics

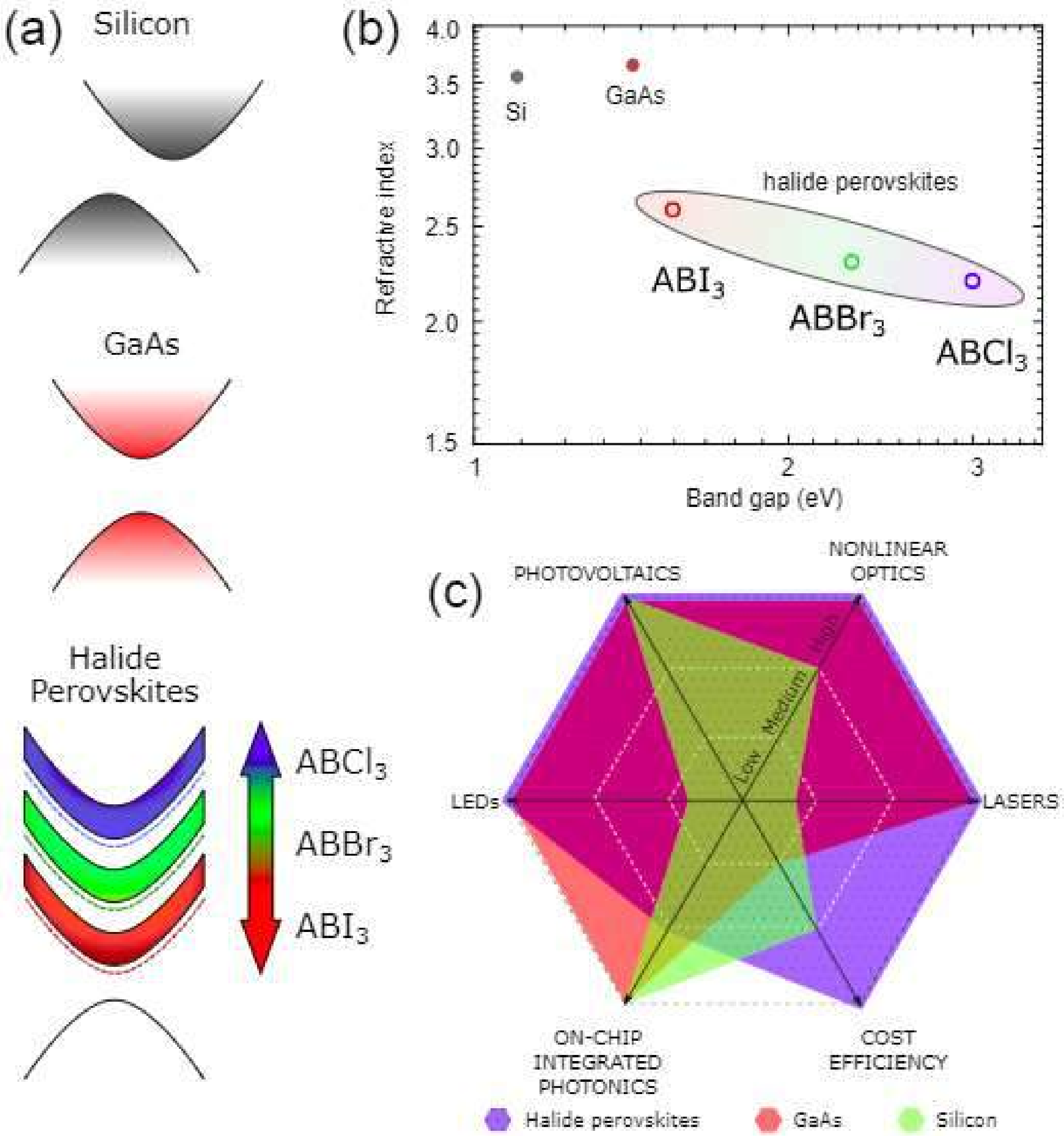

Perovskites based nanophotonics

Why halide perovskites?

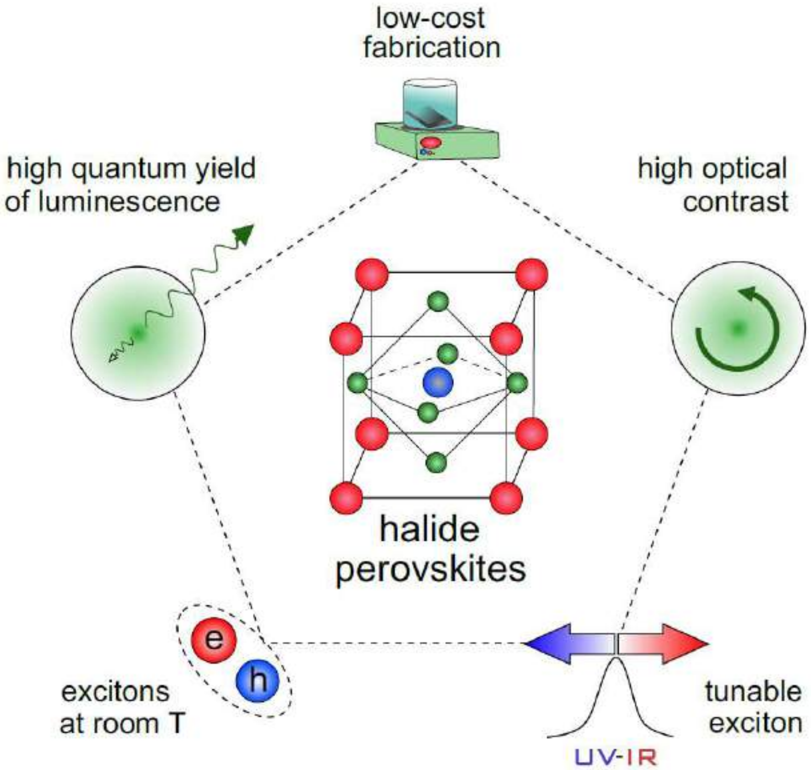

Basic designs

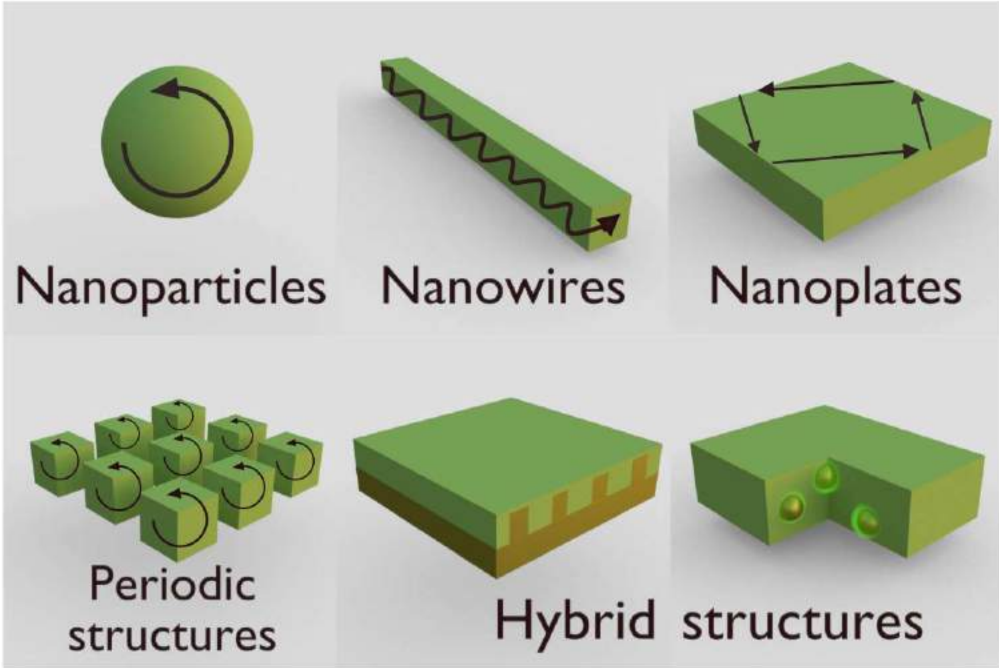

Makarov et al, "Halide-Perovskite Resonant Nanophotonics"
Advanced Optical Materials, 7 (1), 1800784 (2019)

II. Perovskite based nanoscale light sources

Nanoscale tunable light-sources

Ultracompact photonic devices:

- optical modulators
- quantum computing
- gas sensors
- liquid sensors

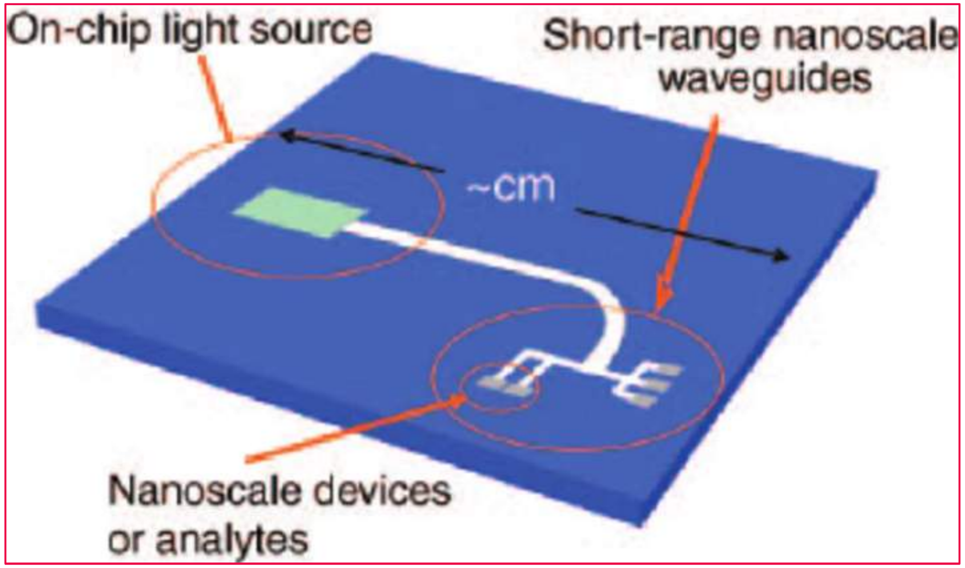

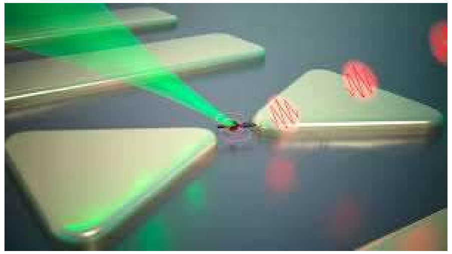

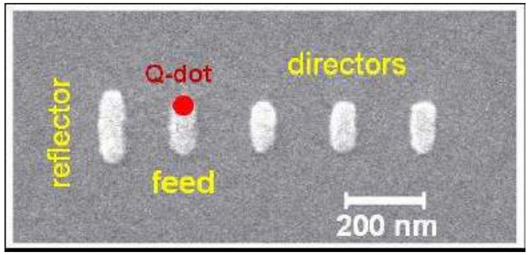

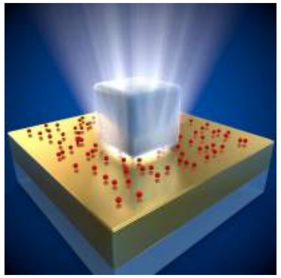

Problems of nanoscale light sources:

- Needs multistep and expensive lithography or epitaxial growth
- Difficult to tune spectrally
- Low quantum efficiencies of luminescence
- Difficult to integrate light source and nanoantenna

Methods of perovskite light sources fabrication

Laser transfer

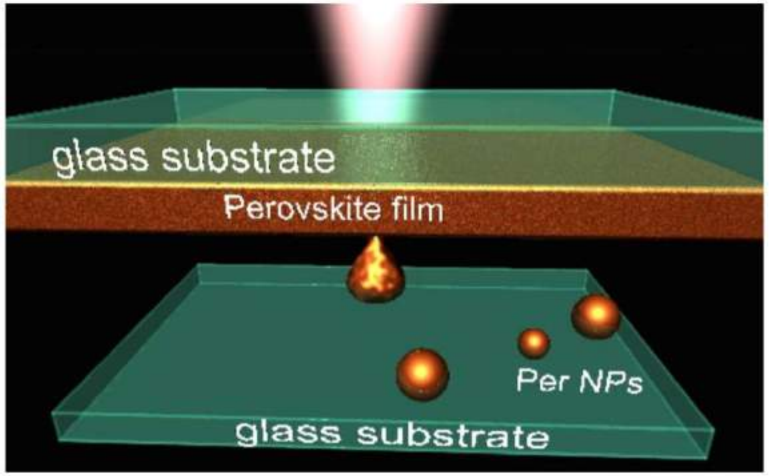

Direct laser imprinting

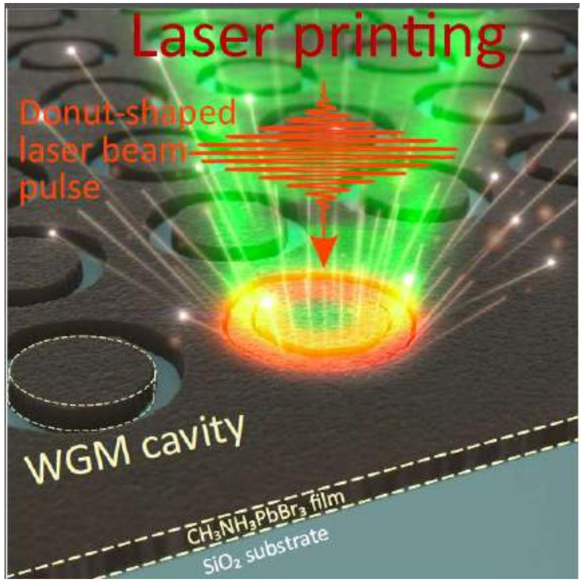

Chemically synthesized

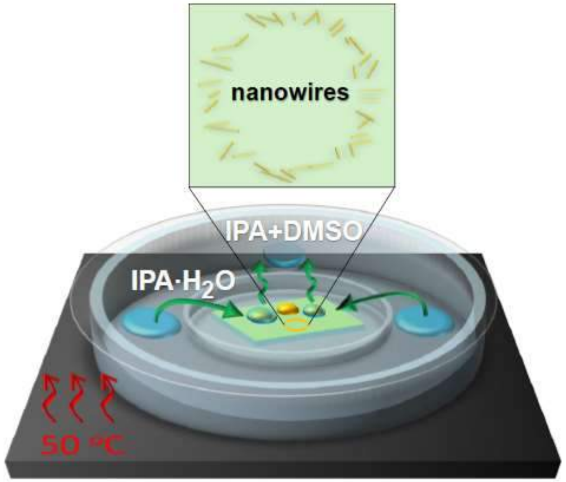

Stamp-imprinted

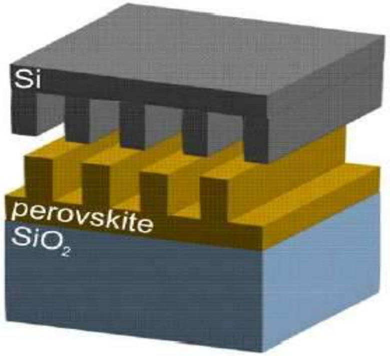

Nanoscale tunable light-sources

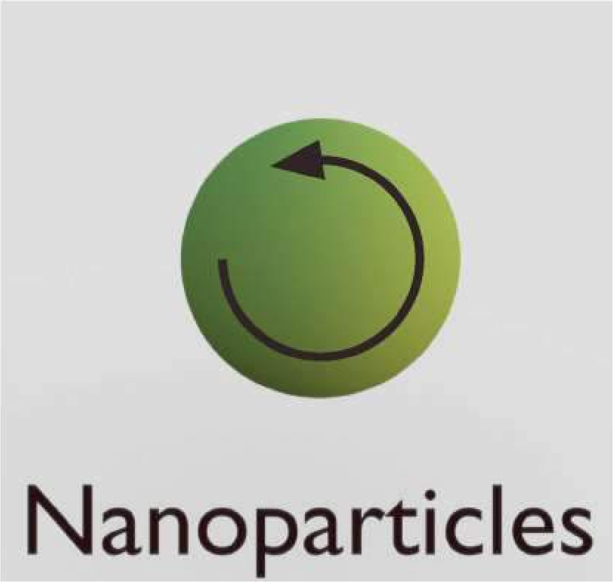

Mie theory

Gustav Mie

$$C_{\rm sca} = \frac{W_{\rm sca}}{I_i} = \frac{2\pi}{k^2}\sum_{n=1}^{\infty}(2n+1)(|a_n|^2 + |b_n|^2)$$

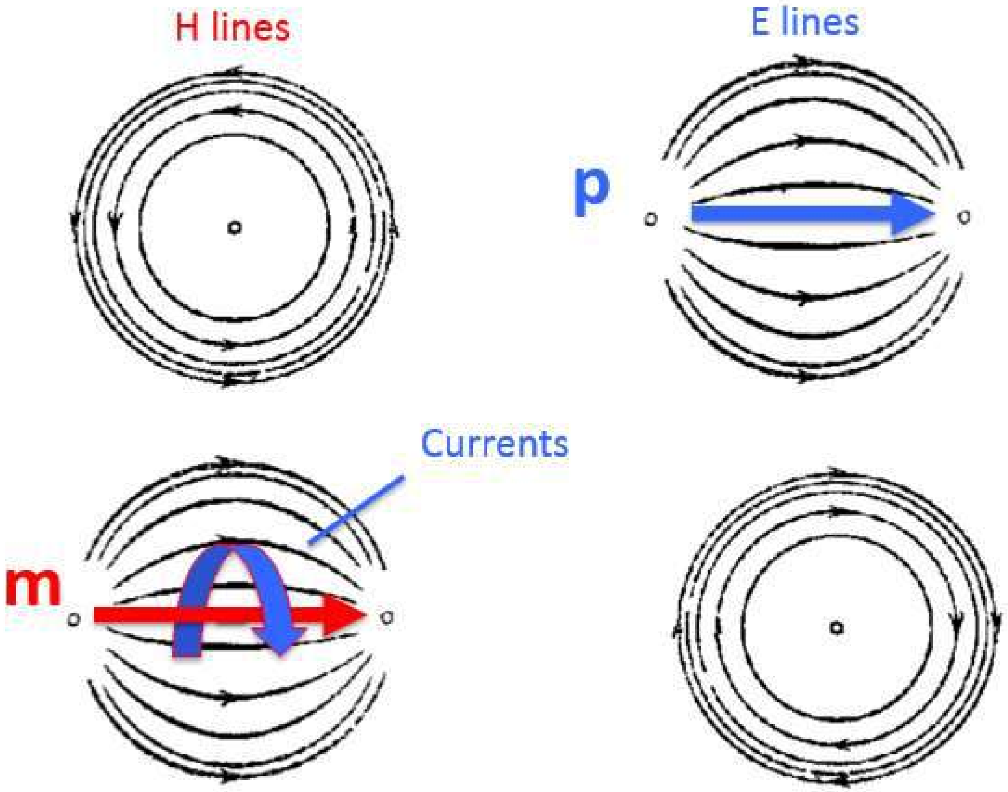

First **electrical** mode

First **magnetic** mode

books Born&Wolf, Bohren&Huffman

ITMO UNIVERSITY
metalab.ifmo.ru

Mie resonances in perovskite NPs

Light scattering on perovskite NPs

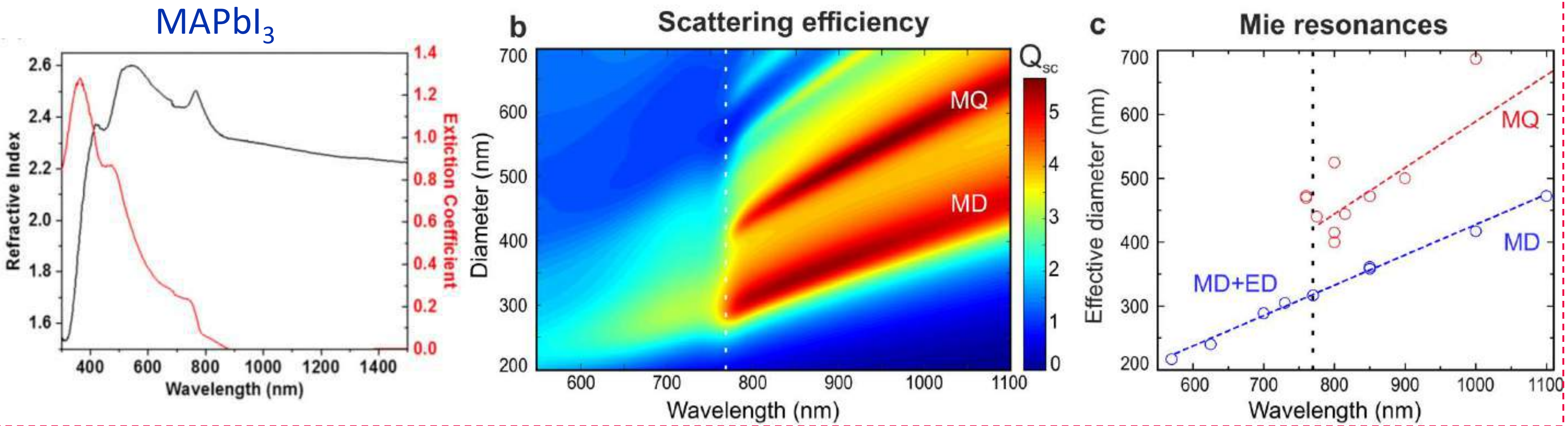

Emission rate enhancement

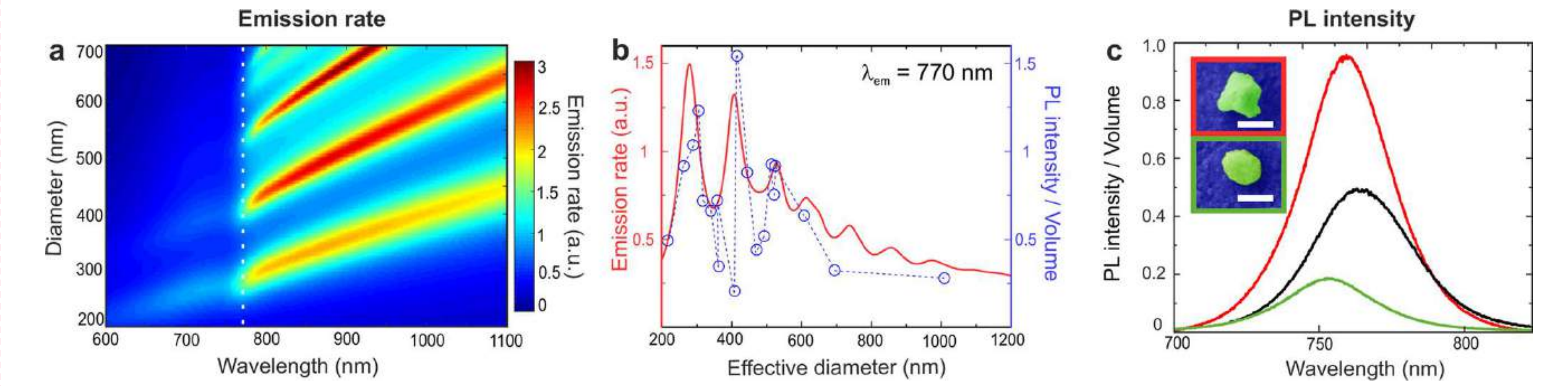

Tiguntseva et al. Nano Lett. 18 (2), 1185-1190 (2018)

ITMO UNIVERSITY
metalab.ifmo.ru

Perovskite resonant nanoparticles

Color change

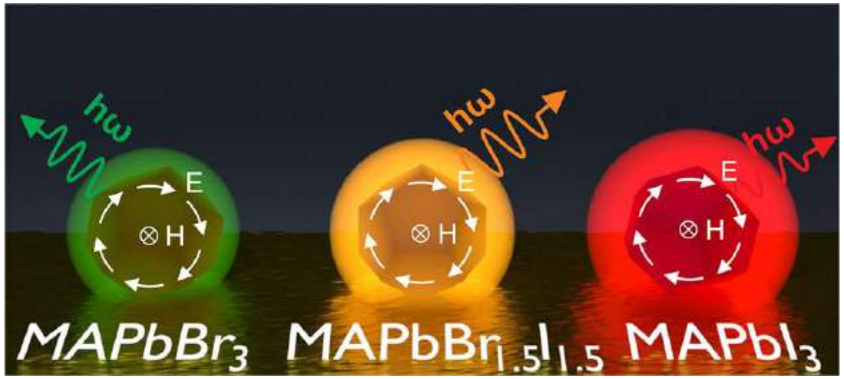

Laser printing

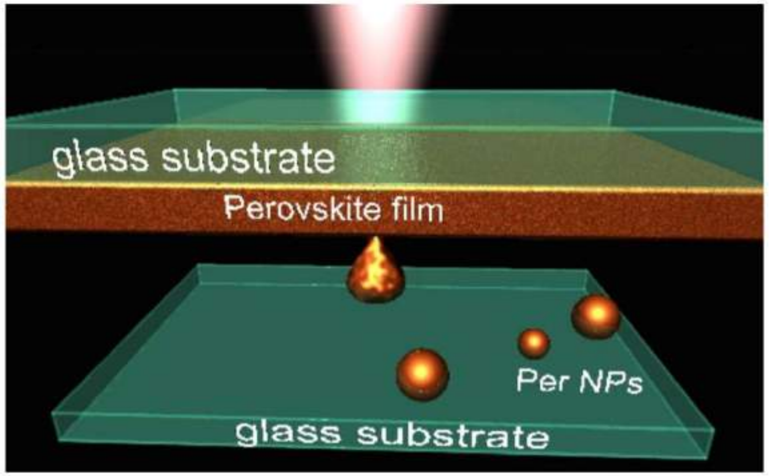

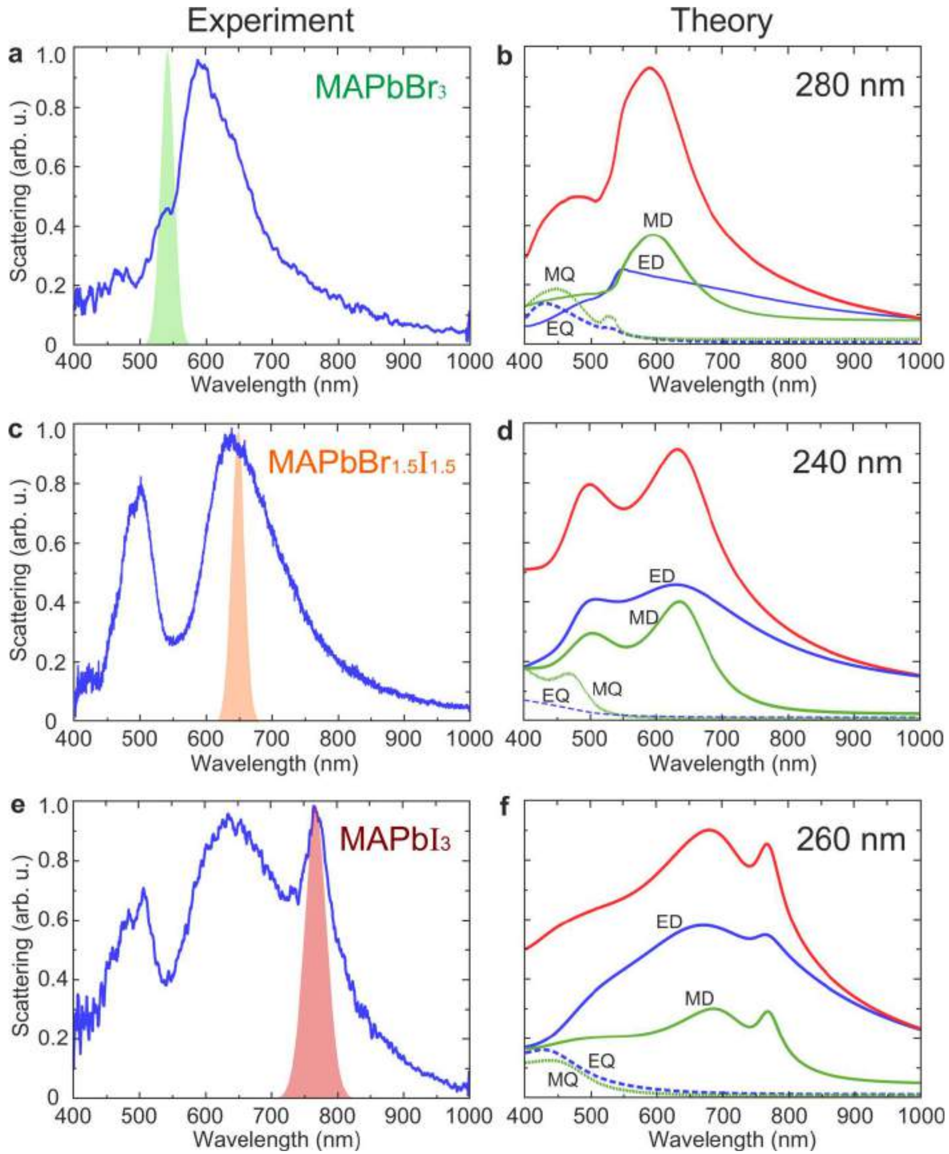

Mie+Exciton=Fano resonance

PHYSICAL REVIEW VOLUME 124, NUMBER 6 DECEMBER 15, 1961

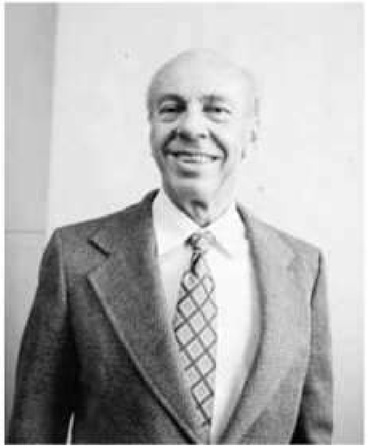

Effects of Configuration Interaction on Intensities and Phase Shifts*

U. Fano
National Bureau of Standards, Washington, D. C.
(Received July 14, 1961)

of phase normalizations. These curves are represented by

$$\frac{|(\Psi_E|T|i)|^2}{|(\psi_E|T|i)|^2}=\frac{(q+\epsilon)^2}{1+\epsilon^2}=1+\frac{q^2-1+2q\epsilon}{1+\epsilon^2}. \qquad (21)$$

This function is plotted in Fig. 1 for a number of values of q, which is regarded as constant in the range of interest. Notice that

$$\frac{(q+\varepsilon)^2}{1+\varepsilon^2}$$

narrow resonance

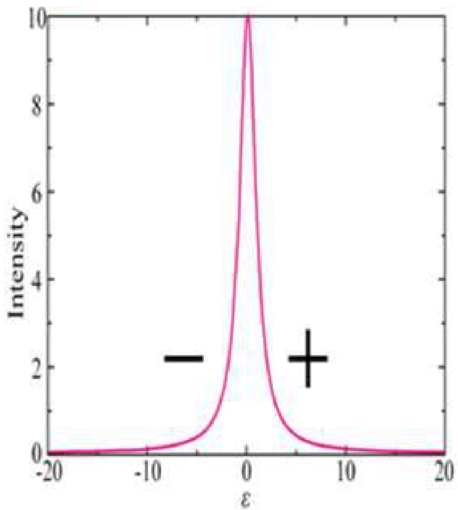

continuum

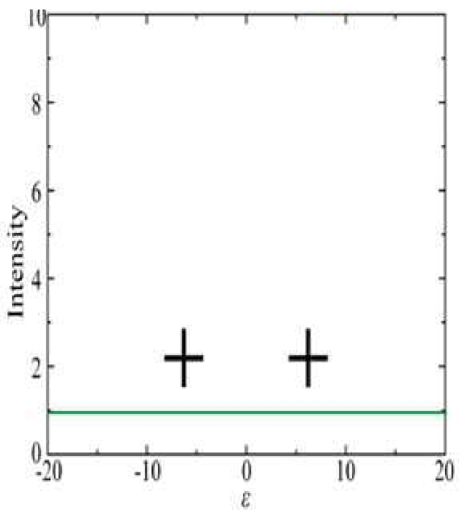

Fano resonance

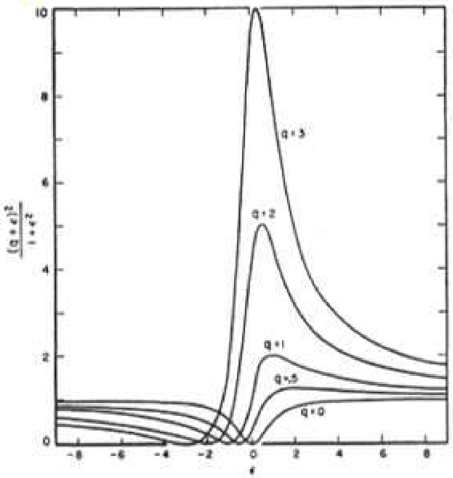

FIG. 1. Natural line shapes for different values of q. (Reverse the scale of abscissas for negative q.)

credits to M.Rybin and M. Limonov

Fano resonance in perovskite NP

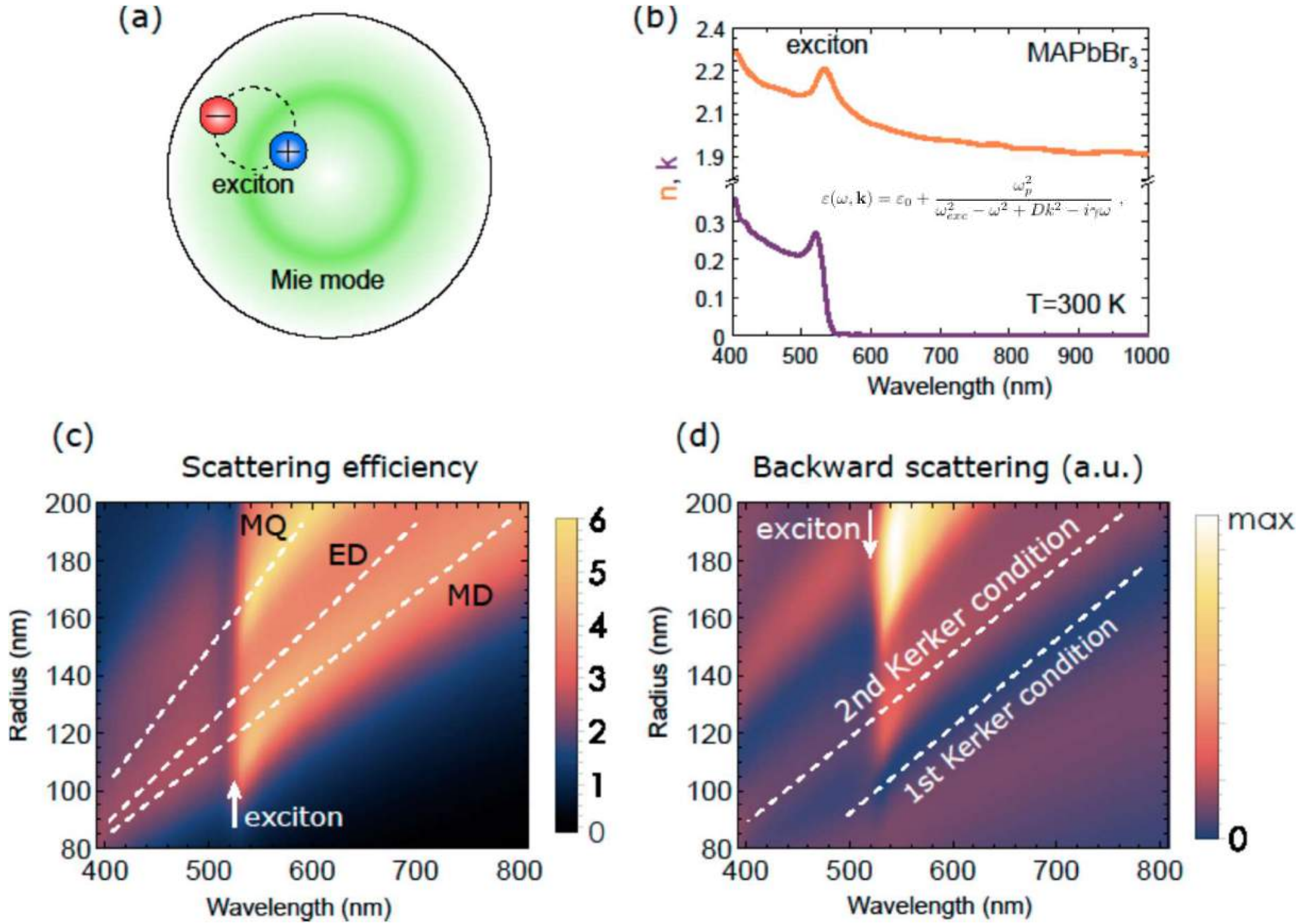

Tiguntseva et al. Nano Lett. 18 (9), 5522-5529 (2018)

Fano resonance in single NP

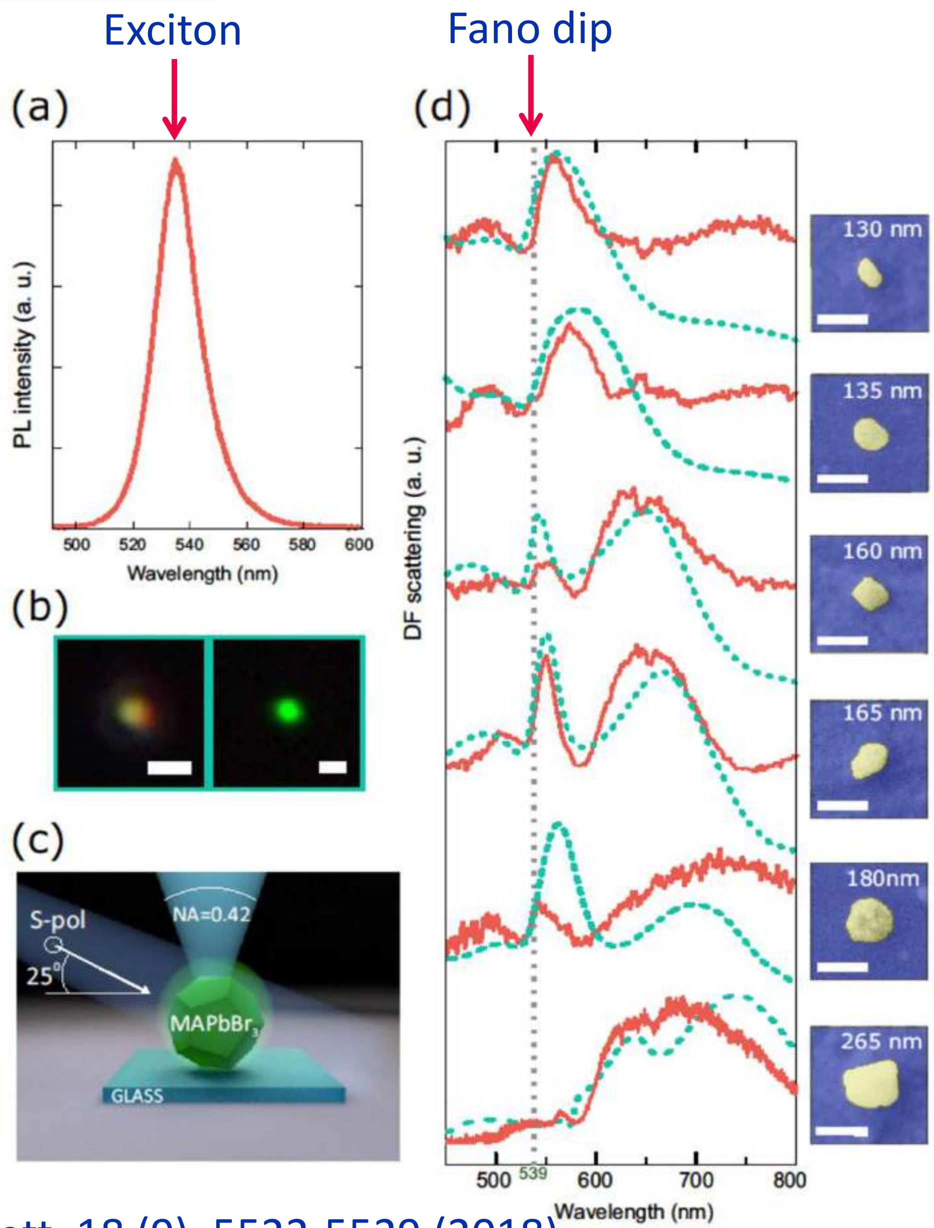

Tiguntseva et al. Nano Lett. 18 (9), 5522-5529 (2018)

Chemical doping in vapor phase

Anion exchange reaction^

y $CsPbBr_3$ (т) + z HCl (г) ⇆ y $CsPbBr_{3-x}Cl_x$ (т) + (z-xy) HCl (г) + xy HBr (г)

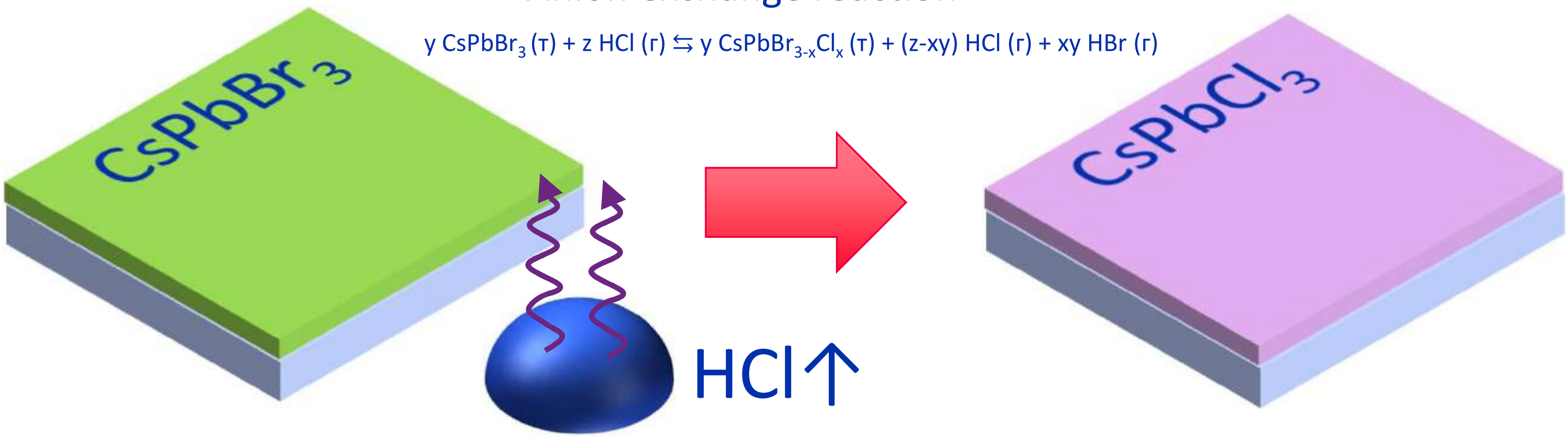

Ellipsometry data

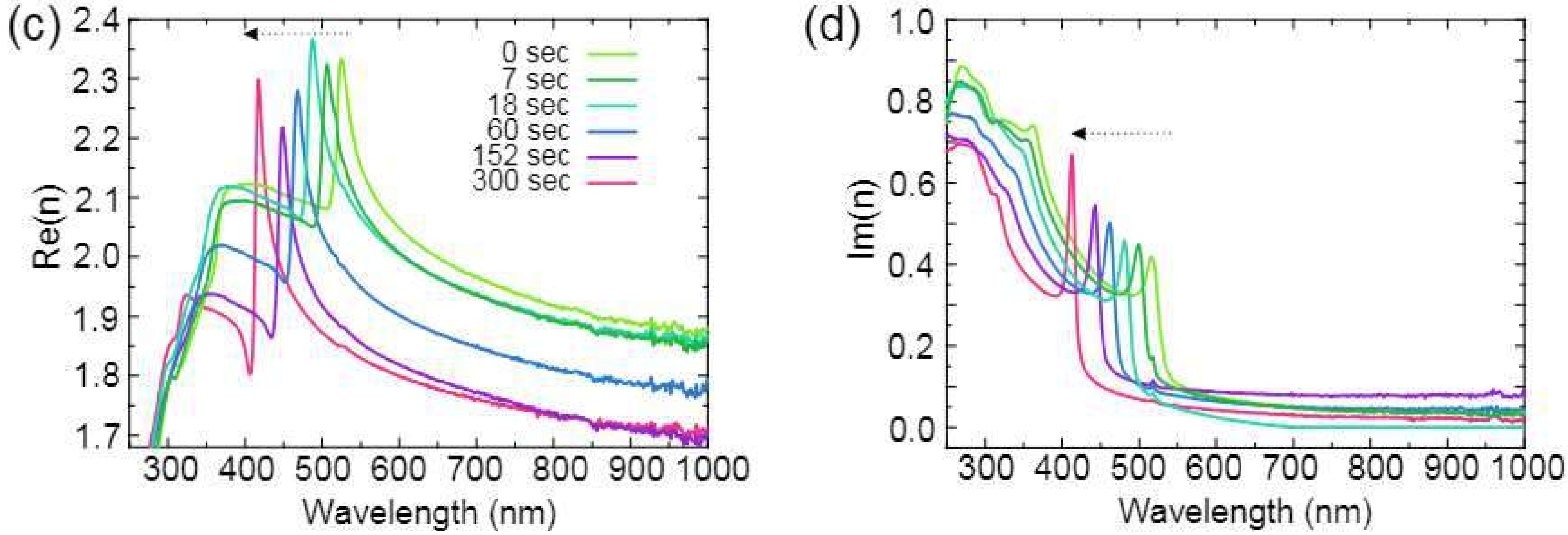

Chemical doping in vapor phase

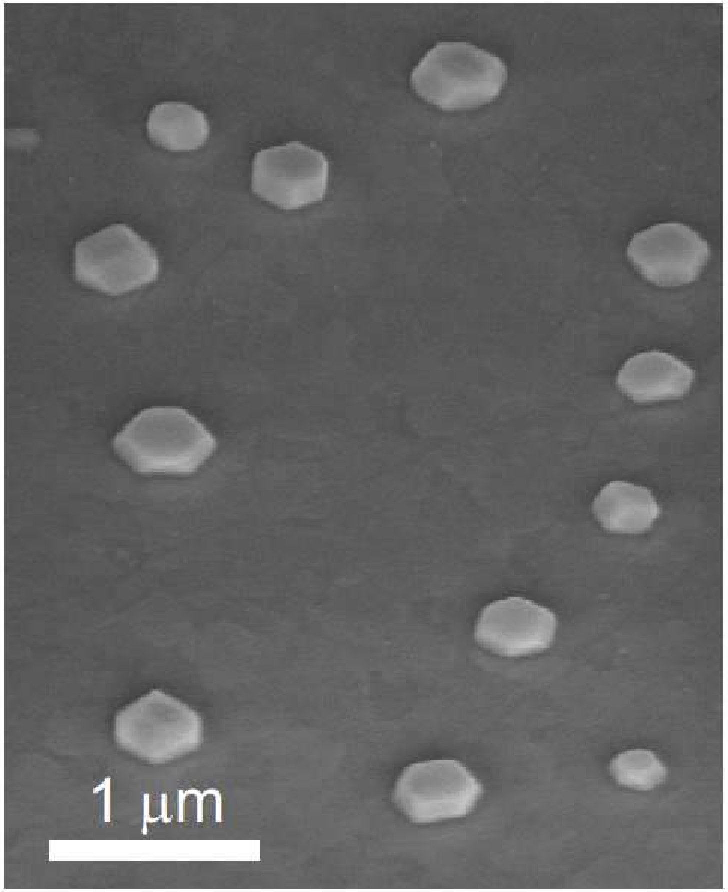

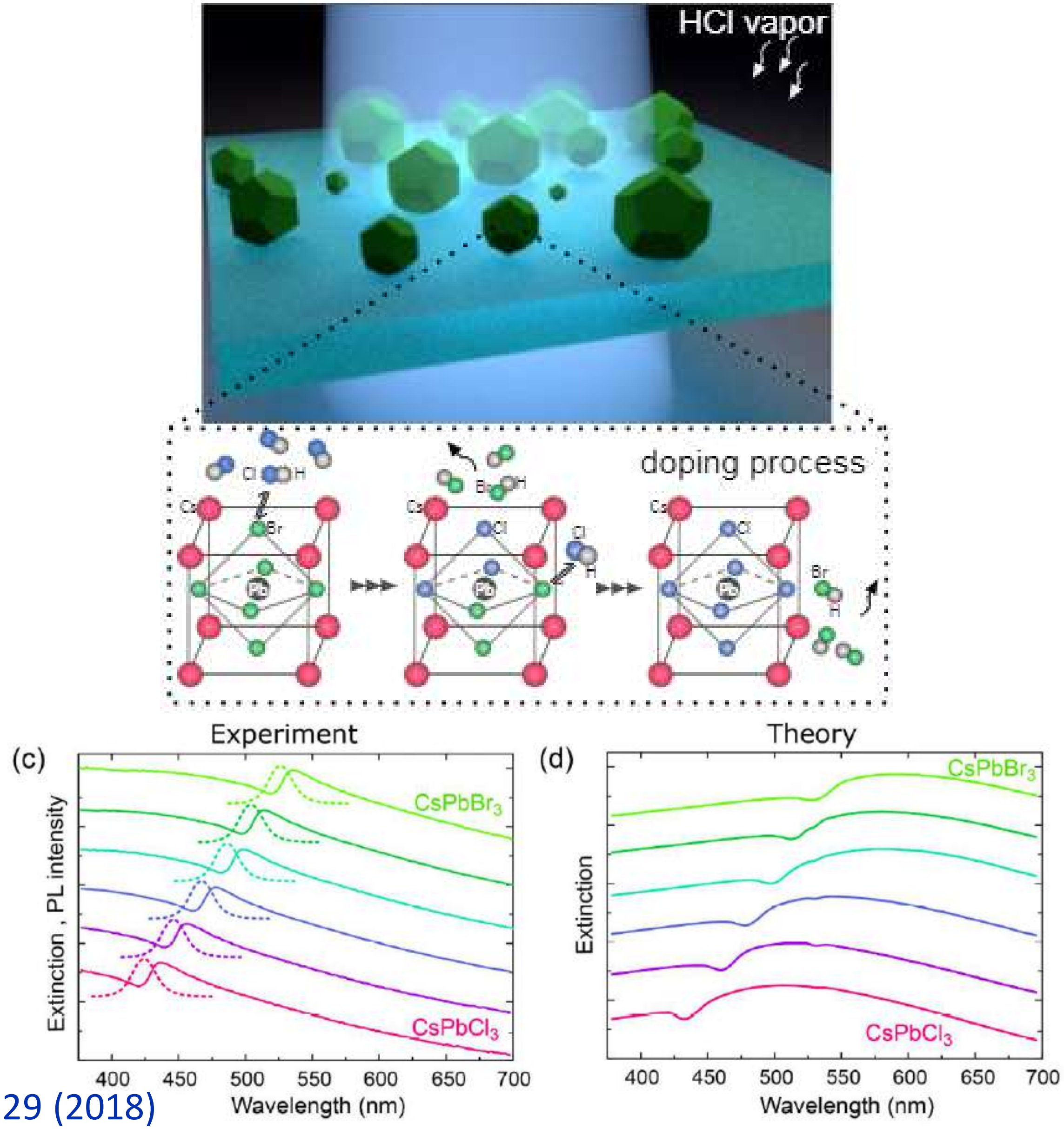

Tiguntseva et al. Nano Lett. 18 (9), 5522-5529 (2018)

Reversible tuning of Fano resonance

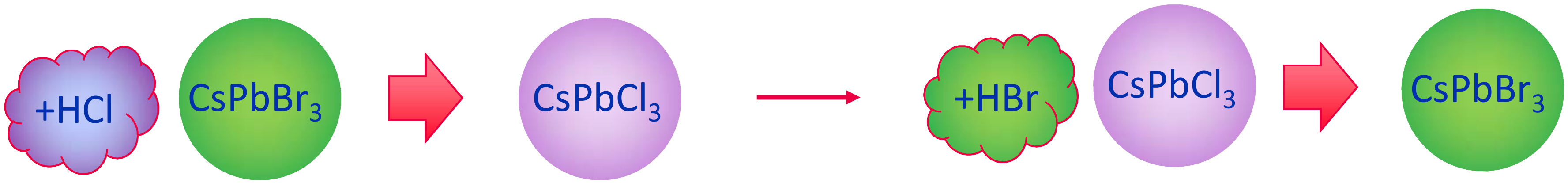

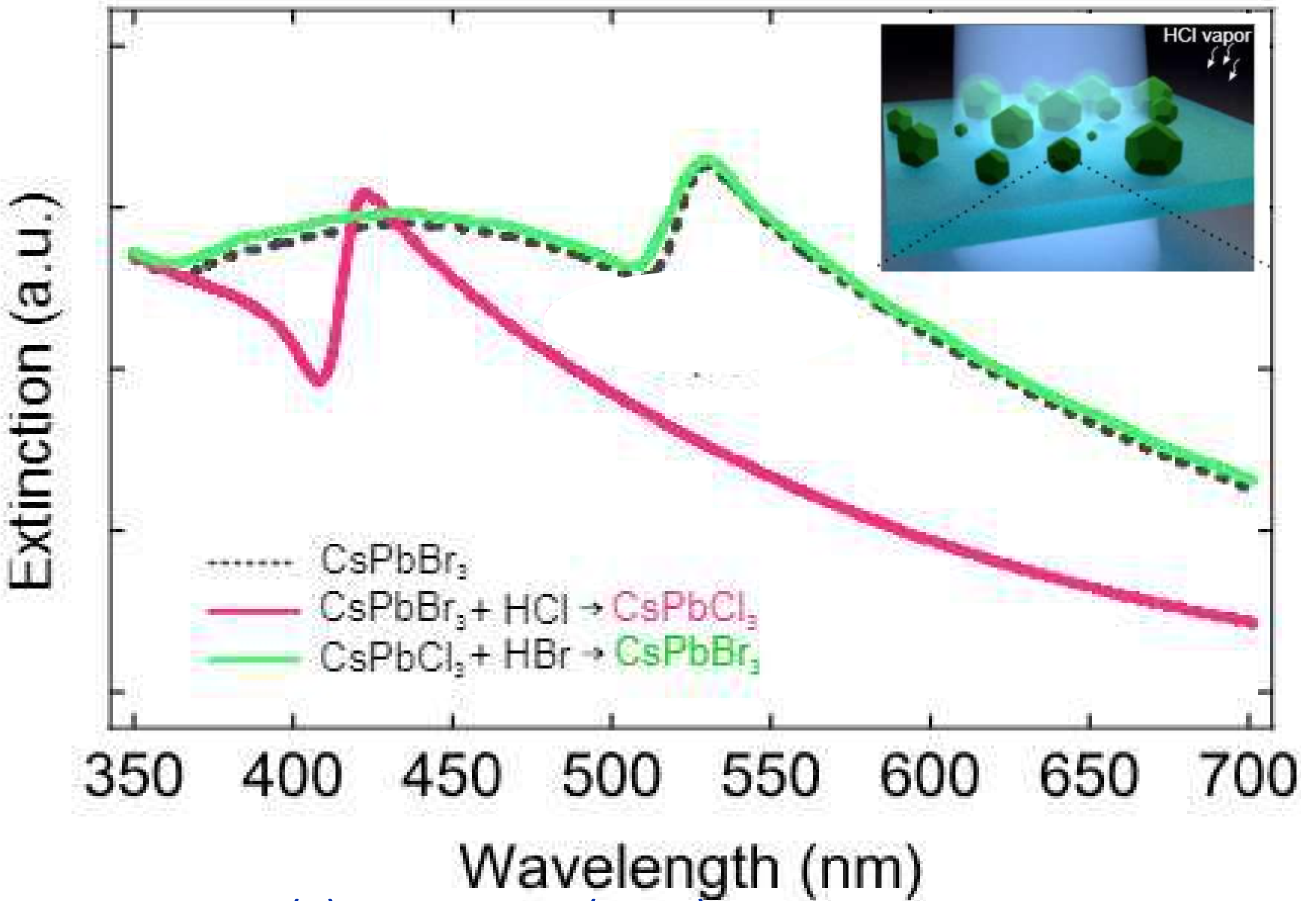

Tiguntseva et al. Nano Lett. 18 (9), 5522-5529 (2018)

Reversible tuning of Fano resonance

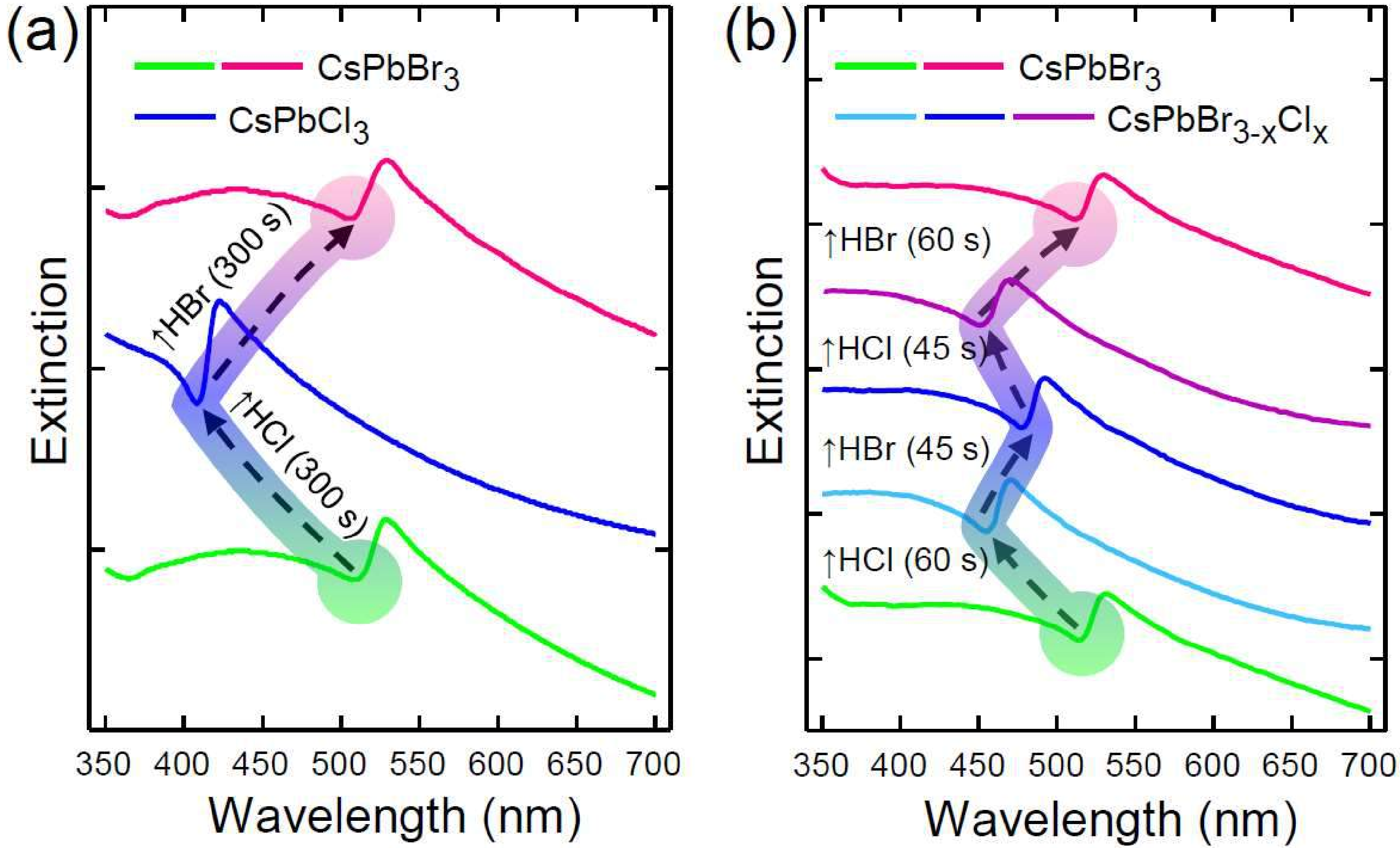

Tiguntseva et al. Nano Lett. 18 (9), 5522-5529 (2018)

Towards to micro- and nano-lasers

$\{D_x, D_y, D_z\} < \lambda$ | $\{D_x, D_z\} < \lambda$ | $D_z < \lambda$

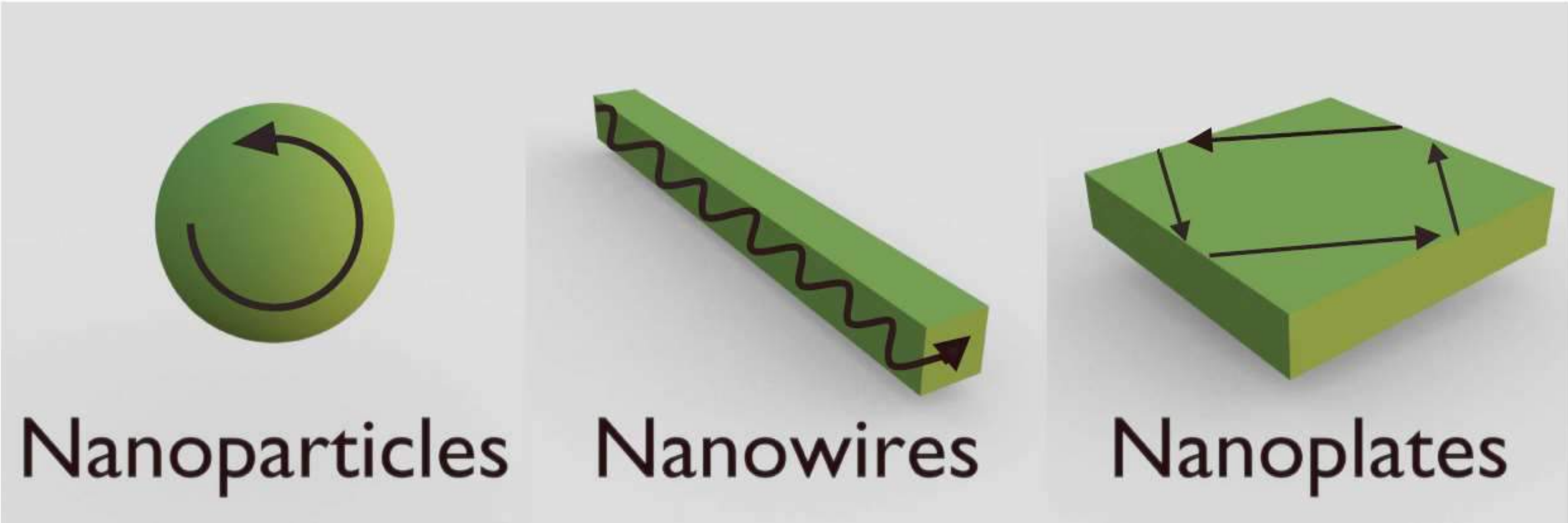

Mie resonances | Fabry-Perot resonances | Whispering Gallery modes

10 — Quality factor — 10^4

Towards to micro- and nano-lasers

- ✓ High gain
- ✓ Easy to fabricate
- ✓ High quality
- ✓ Tunability

Absorption/gain ~ 10^4 - 10^5 cm^{-1}

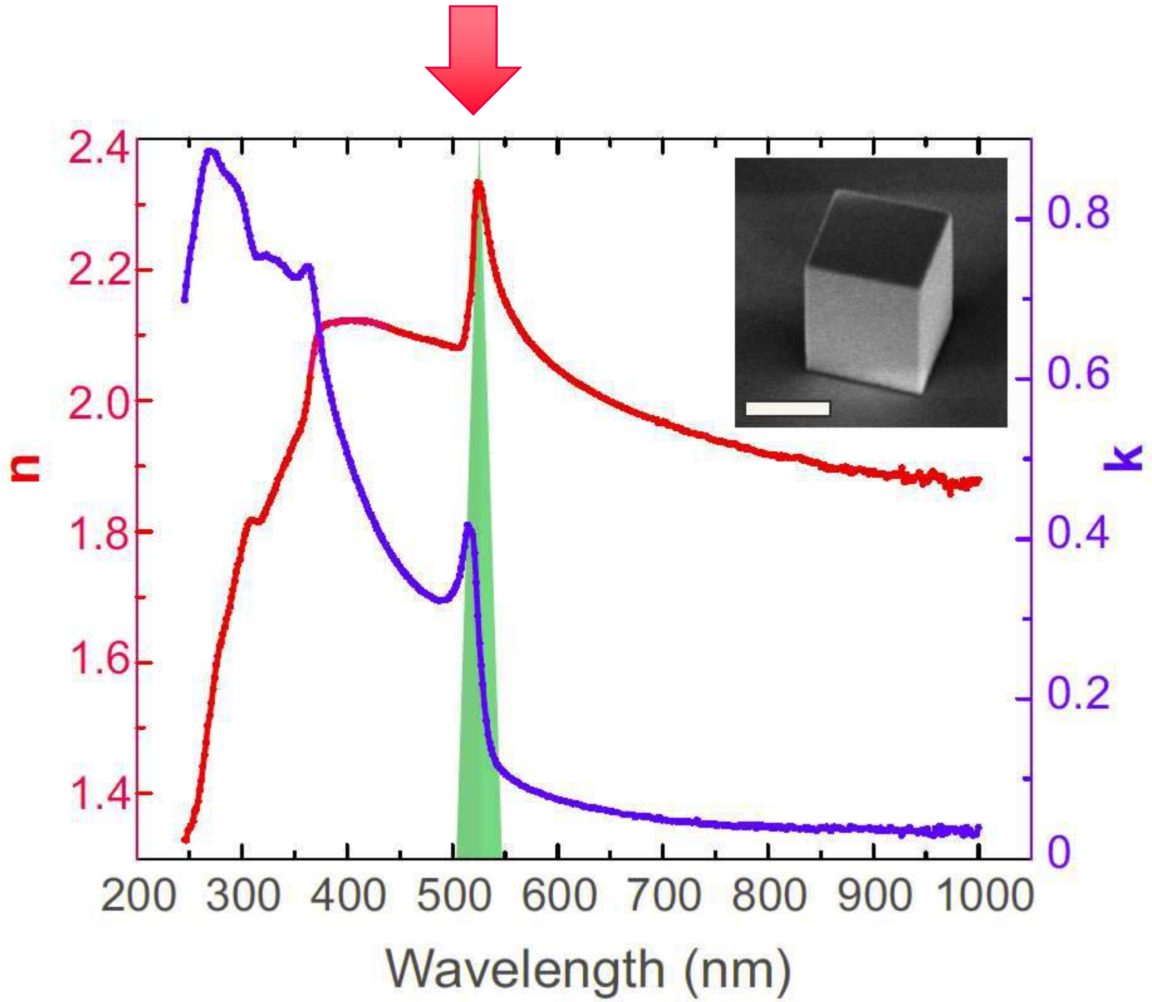

Few-minutes chemical synthesis

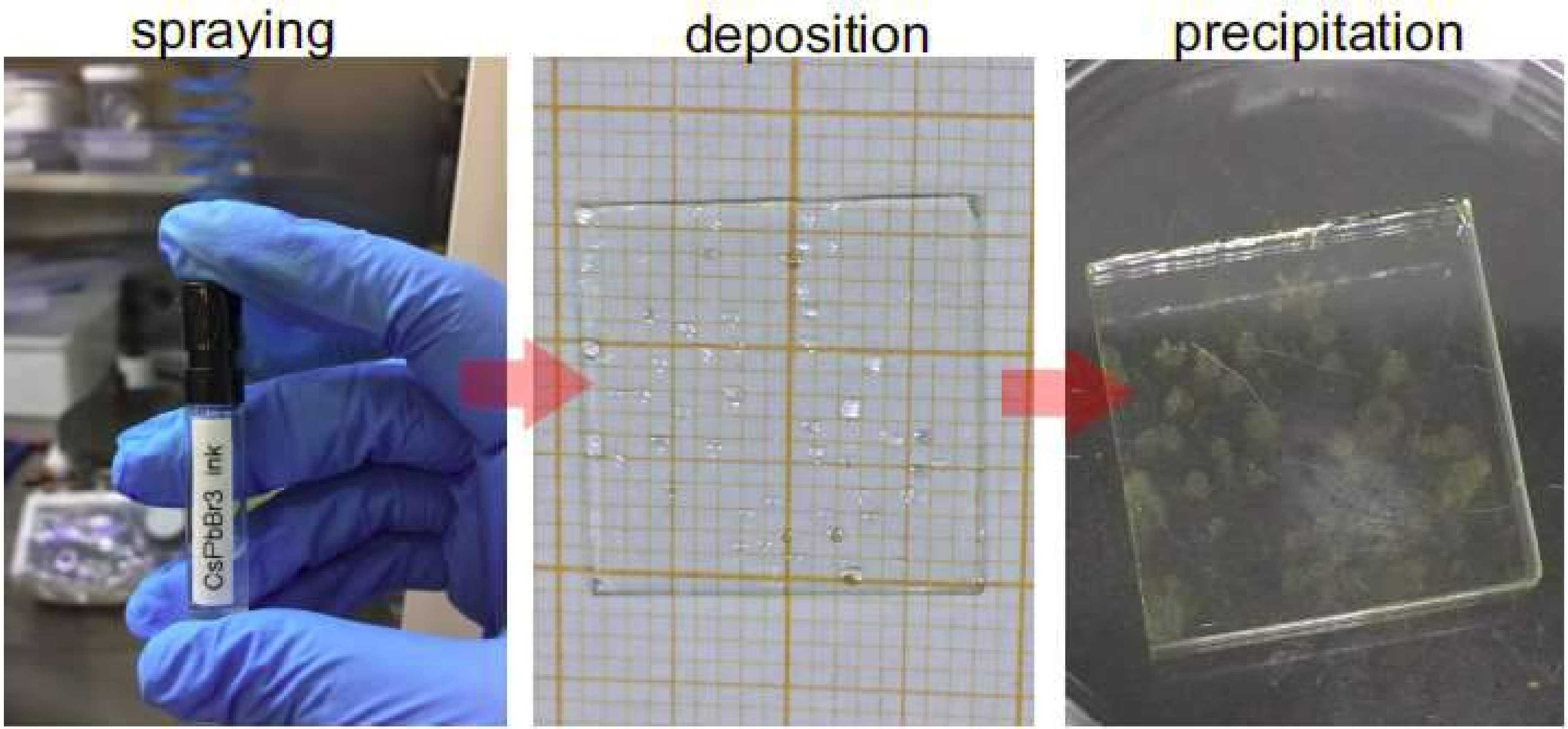

Pushkarev et al. ACS Appl. Mater. Interfaces, 11 (1), 1040–1048 (2019)

Lasing properties

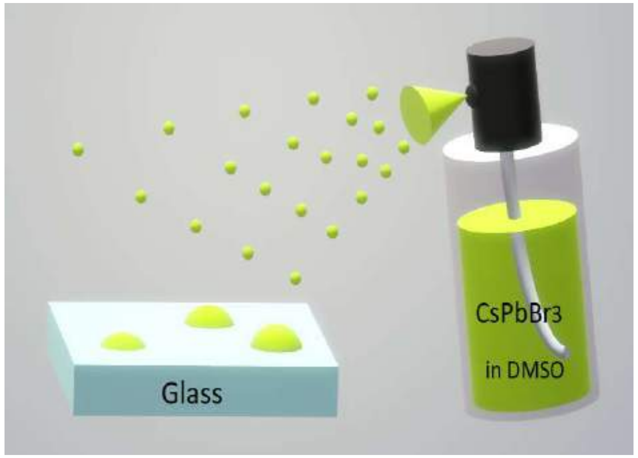

5 min

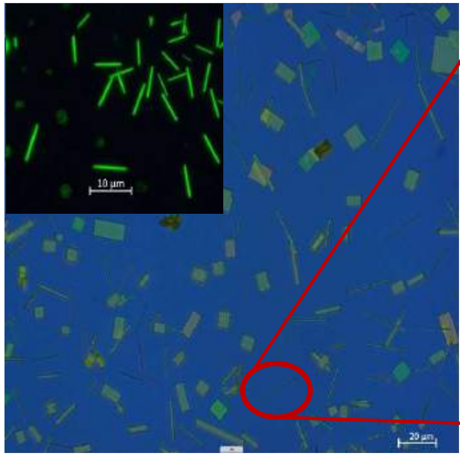

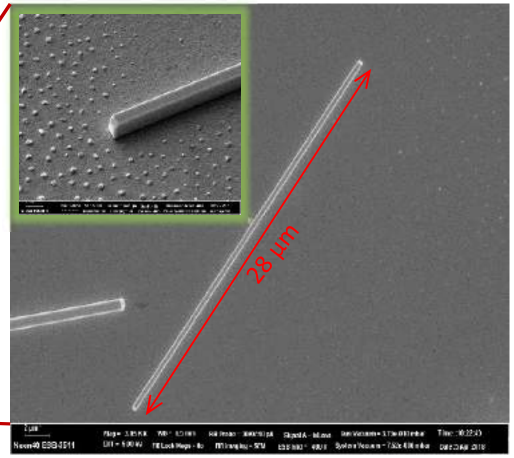

$CsPbBr_3$

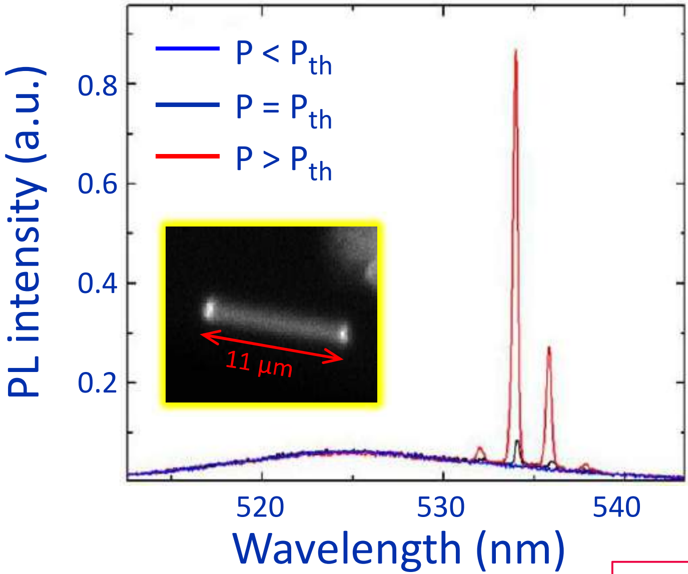

λ_{max}=534 nm
$\delta\lambda$=0.25 nm
Q = 2100
F_{th} ~ 50 uJ/cm2

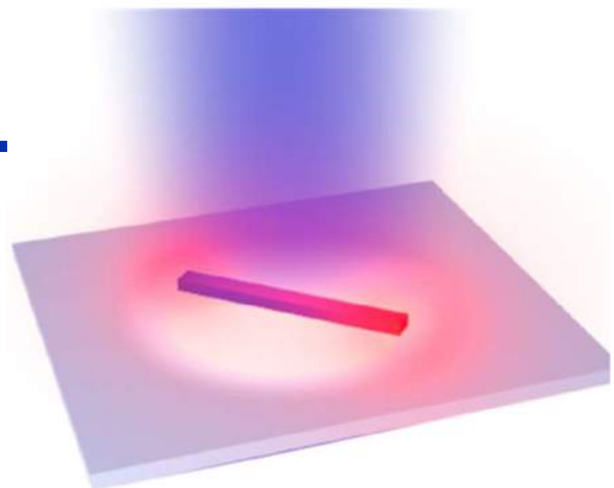

Problem: difficult to control the position!

Laser printing of perovskite lasers

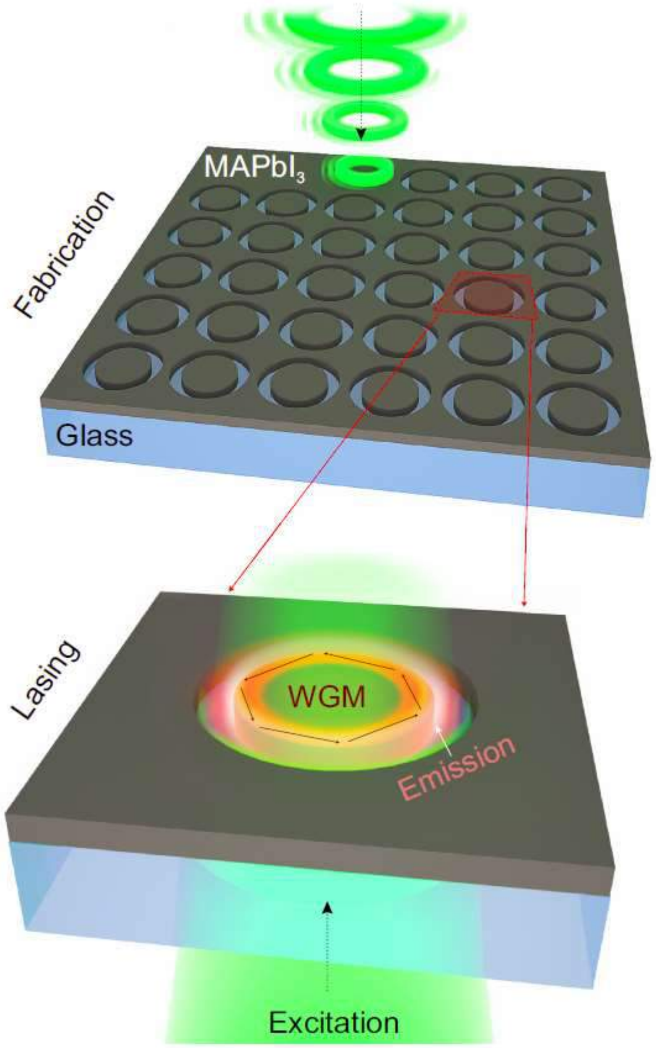

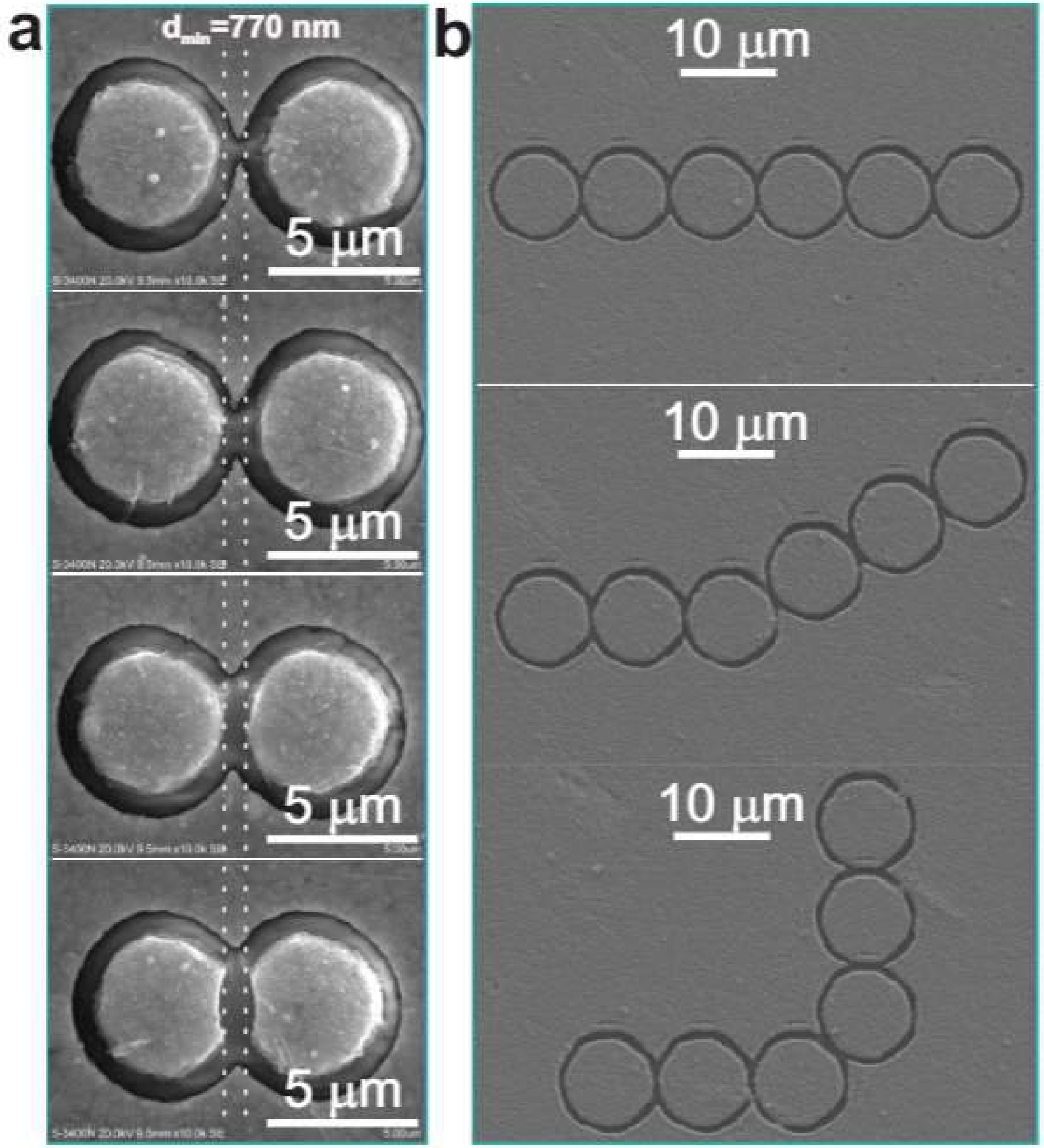

Large-scale fabrication

$MAPbI_3$

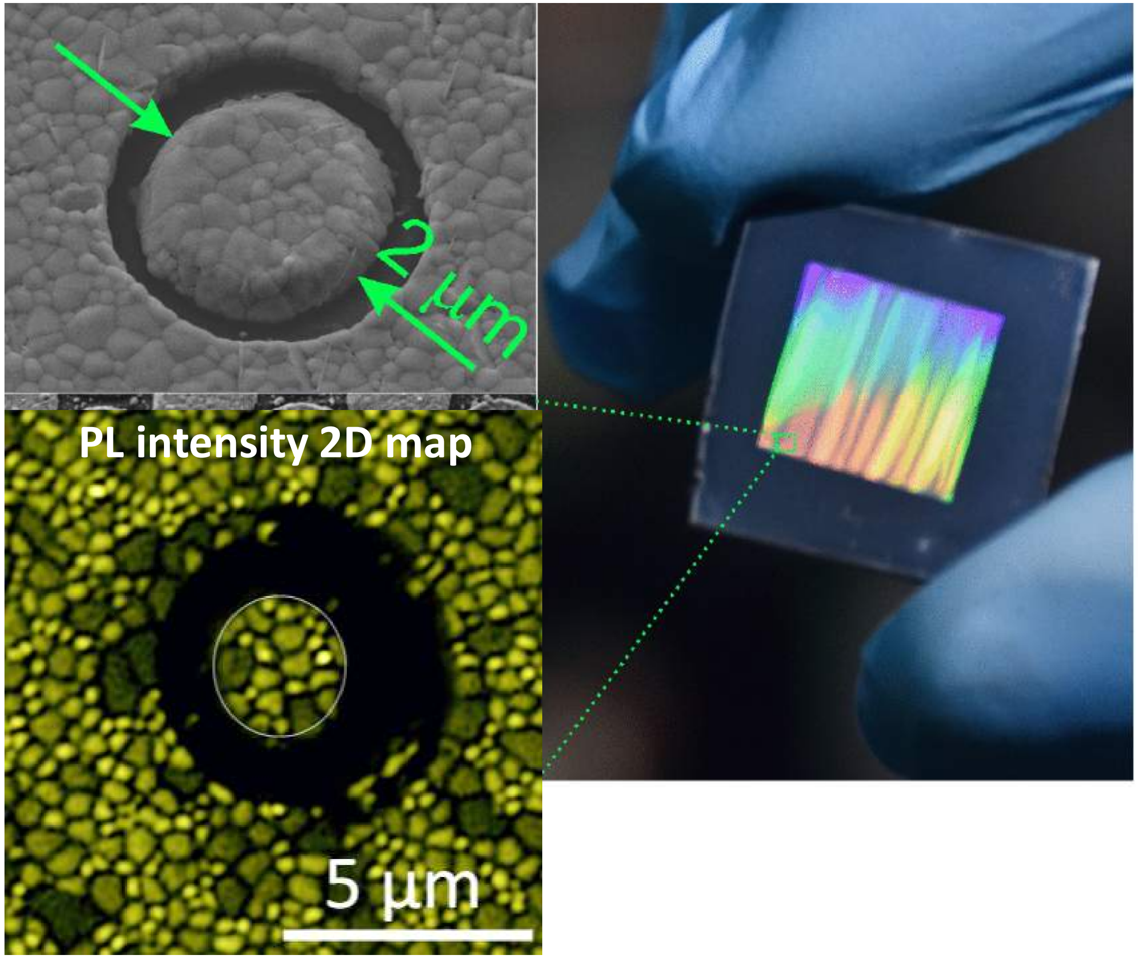

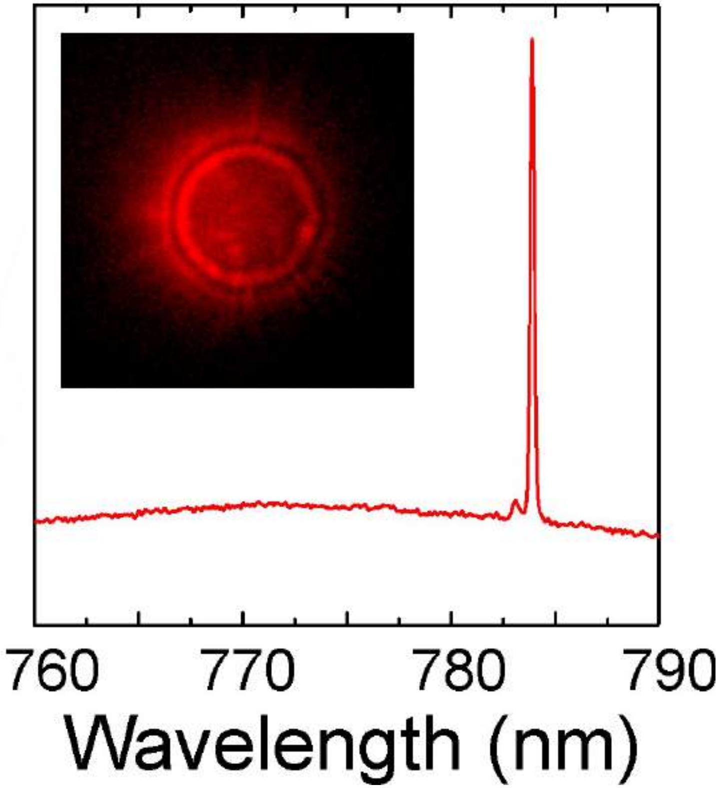

Perovskite is a defect-tolerant material!

Zhizhchenko et al. ACS Nano doi:10.1021/acsnano.8b08948 (2019)

Lasing properties: single mode & room T

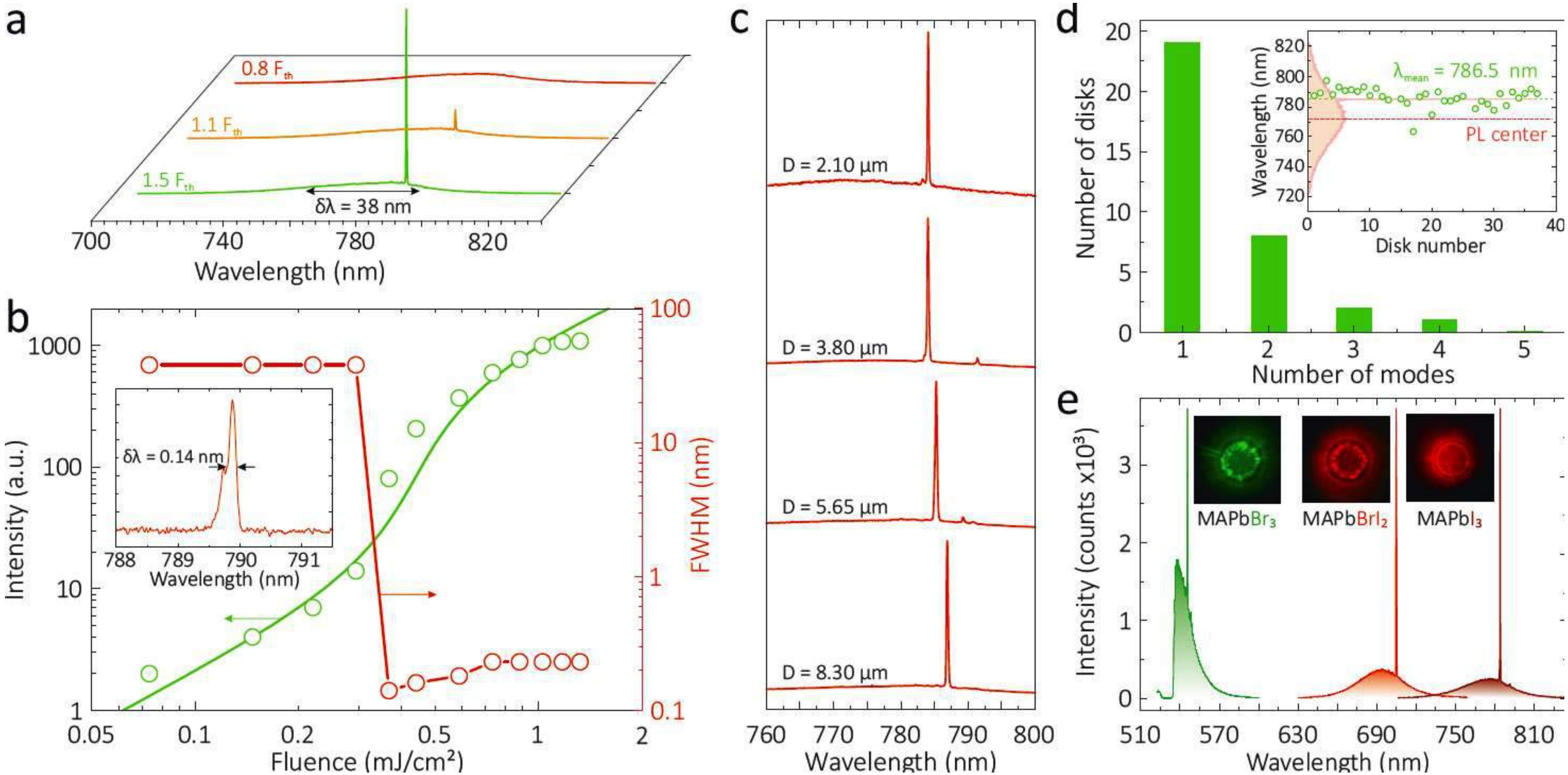

ns-threshold: ~ 200 μJ/cm^2
fs-threshold: < 10 μJ/cm^2

Zhizhchenko et al. ACS Nano doi:10.1021/acsnano.8b08948 (2019)

Modeling

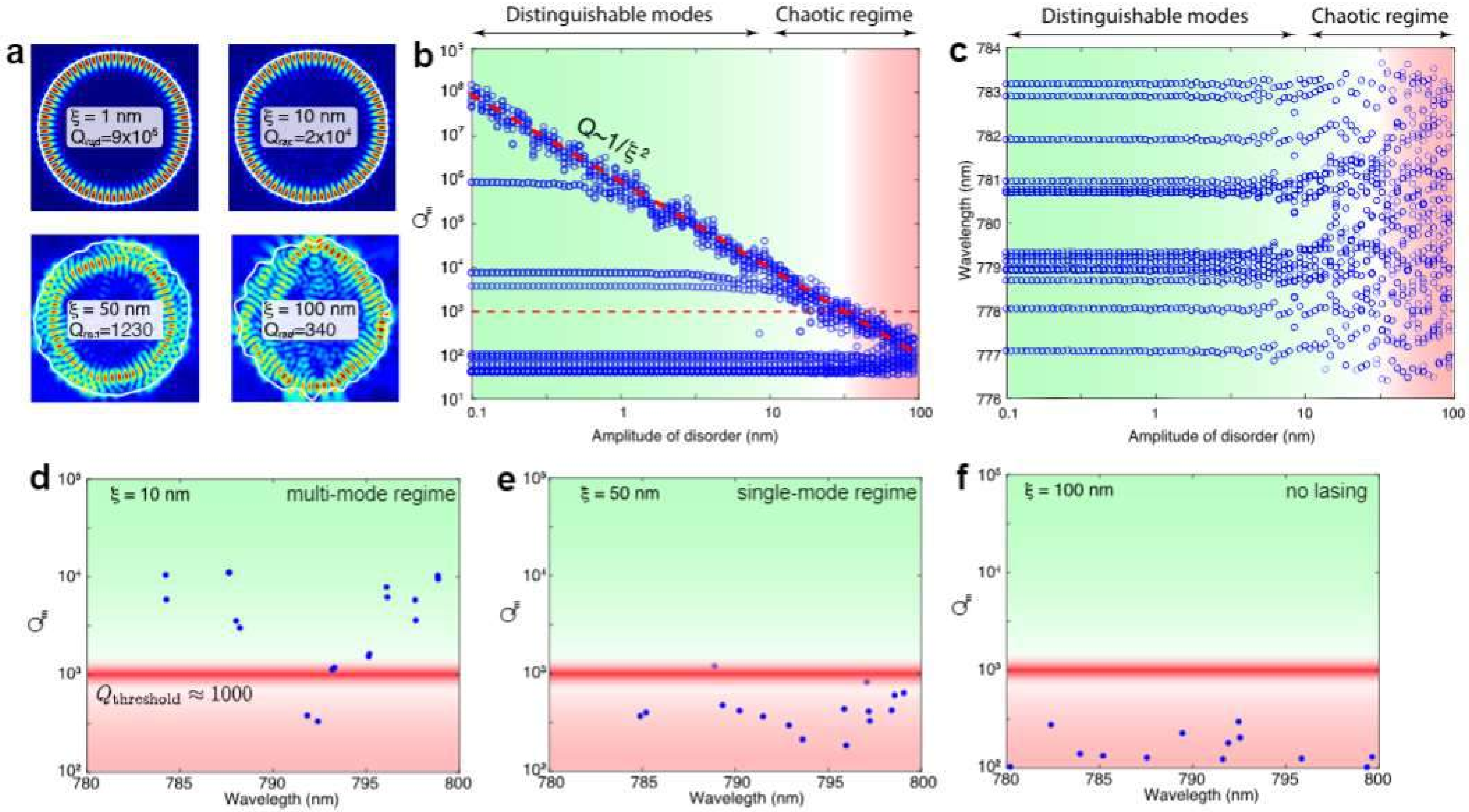

Roughness selects the WGM modes

Zhizhchenko et al. ACS Nano doi:10.1021/acsnano.8b08948 (2019)

ITMO UNIVERSITY
metalab.ifmo.ru

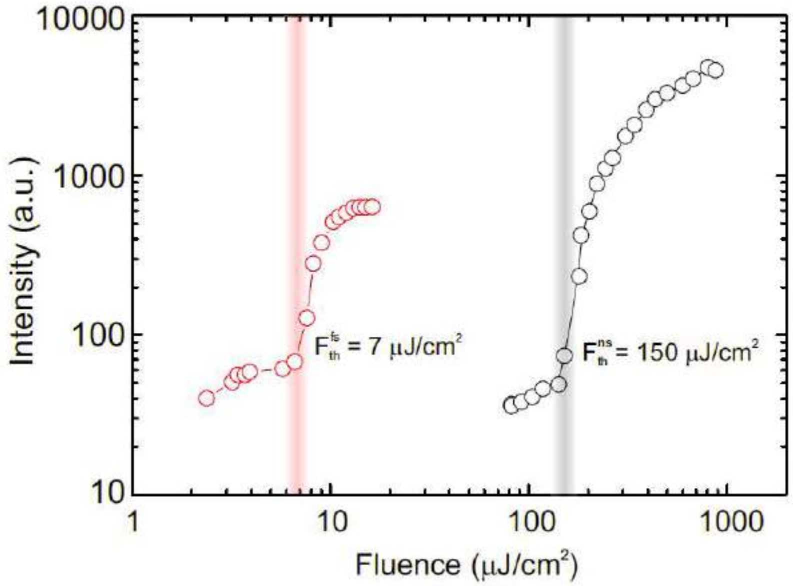

$$\frac{dn}{dt} = \eta_p \frac{P}{\hbar\omega_p V_a} - R_{nr}(n) - R_{sp}(n) - R_{st}(n)s$$

$$\frac{ds}{dt} = -\frac{s}{\tau_p} + \Gamma\beta_{sp}R_{sp}(n) + \Gamma R_{st}(n)s,$$

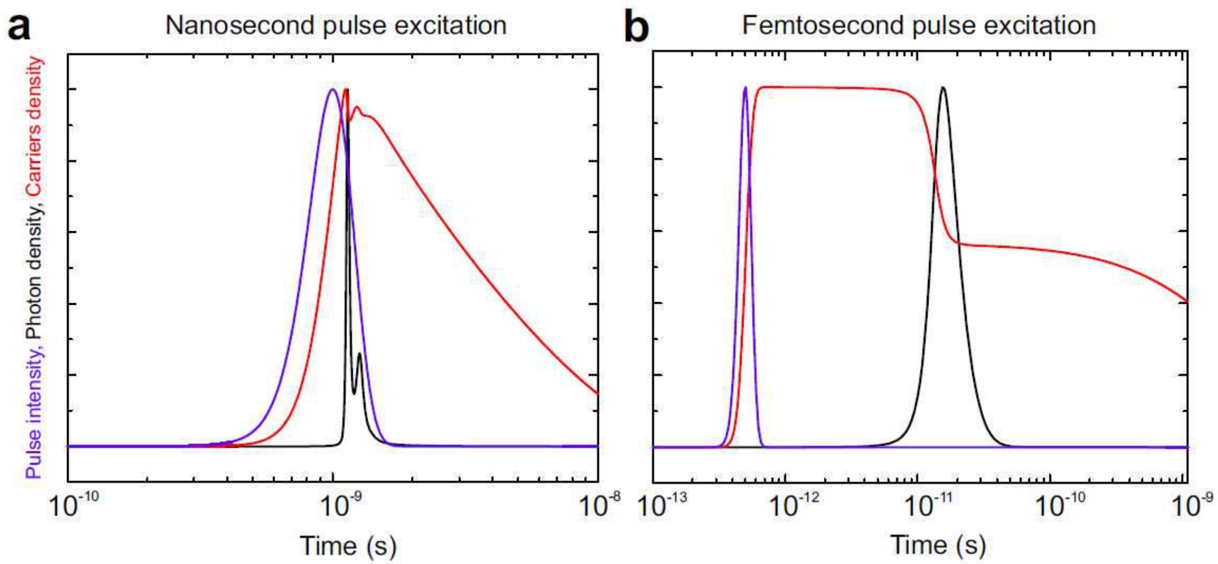

Conclusion

- ✓ Reversibly tunable perovskite nanoantennas

  Tiguntseva et al. Nano Lett. 18 (2), 1185-1190 (2018)

  Tiguntseva et al. Nano Lett. 18 (9), 5522-5529 (2018)

- ✓ Extremely fast method of nanowire lasers synthesis

  Pushkarev et al. ACS Appl. Mater. Interfaces, 11 (1), 1040–1048 (2019)

- ✓ Large-scale laser printing of perovskite microlasers

  Zhizhchenko et al. ACS Nano doi:10.1021/acsnano.8b08948 (2019)

- ✓ All-dielectric nanolasers…

  Tiguntseva et al. (in progress)

Review: Makarov et al, “Halide-Perovskite Resonant Nanophotonics”
Advanced Optical Materials, 7 (1), 1800784 (2019)

ITMO UNIVERSITY

Thank you for your attention!

Made by Pushkarev

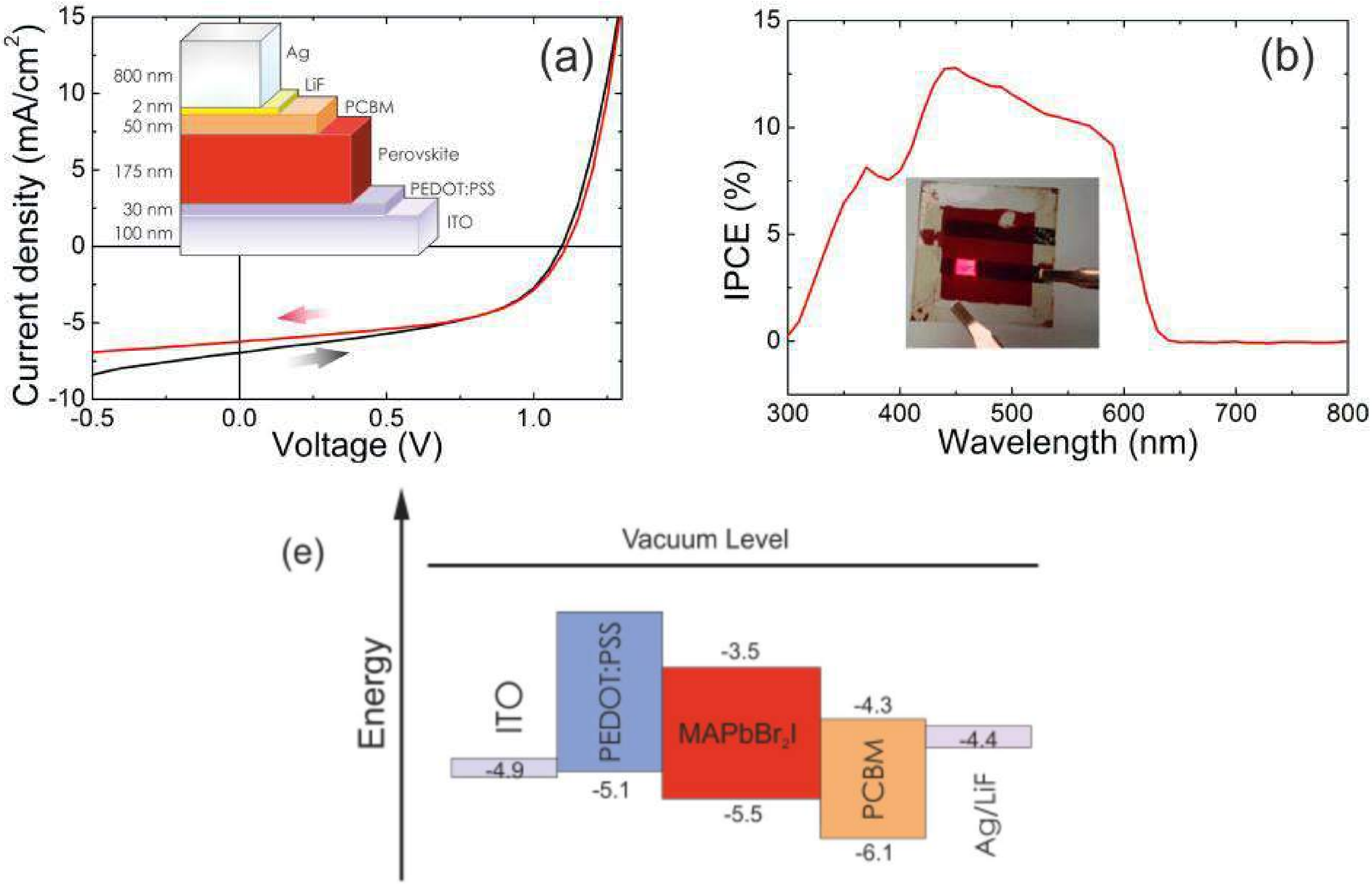

Gets et al. Applied Surface Science 476, 486-492 (2019)

Nanoimprint lithography

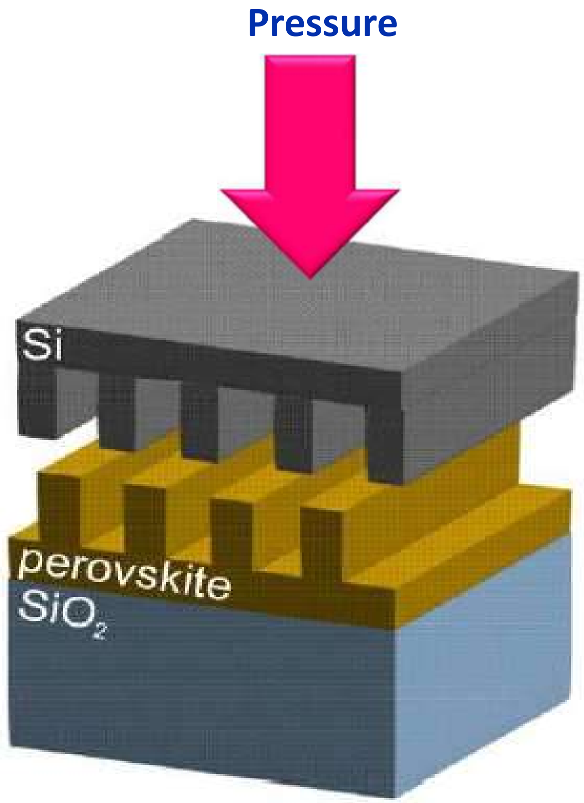

Scheme of nanoimprint lithography process

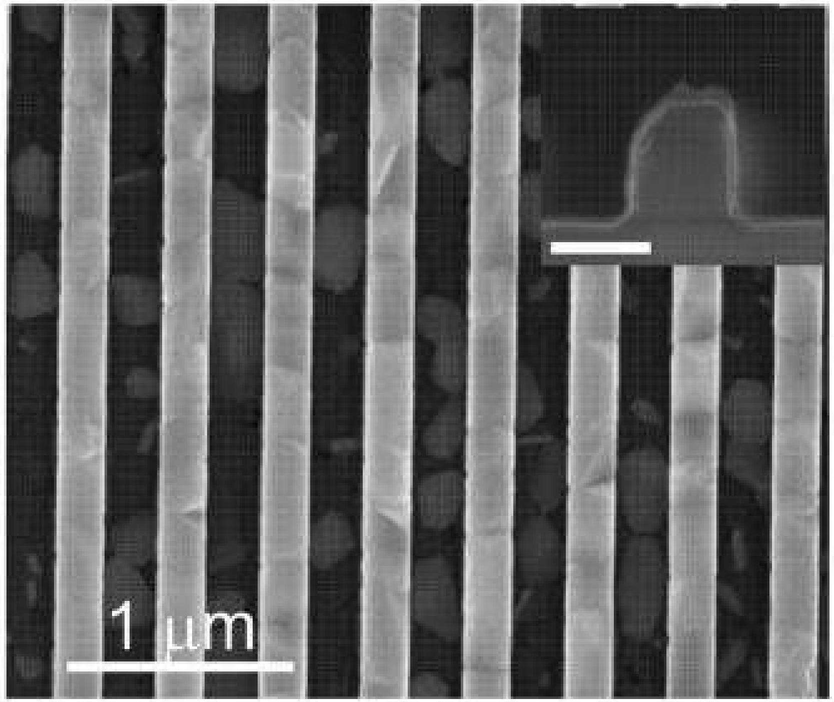

SEM image of film structure

Photoluminescence behavior

$MAPbI_3$

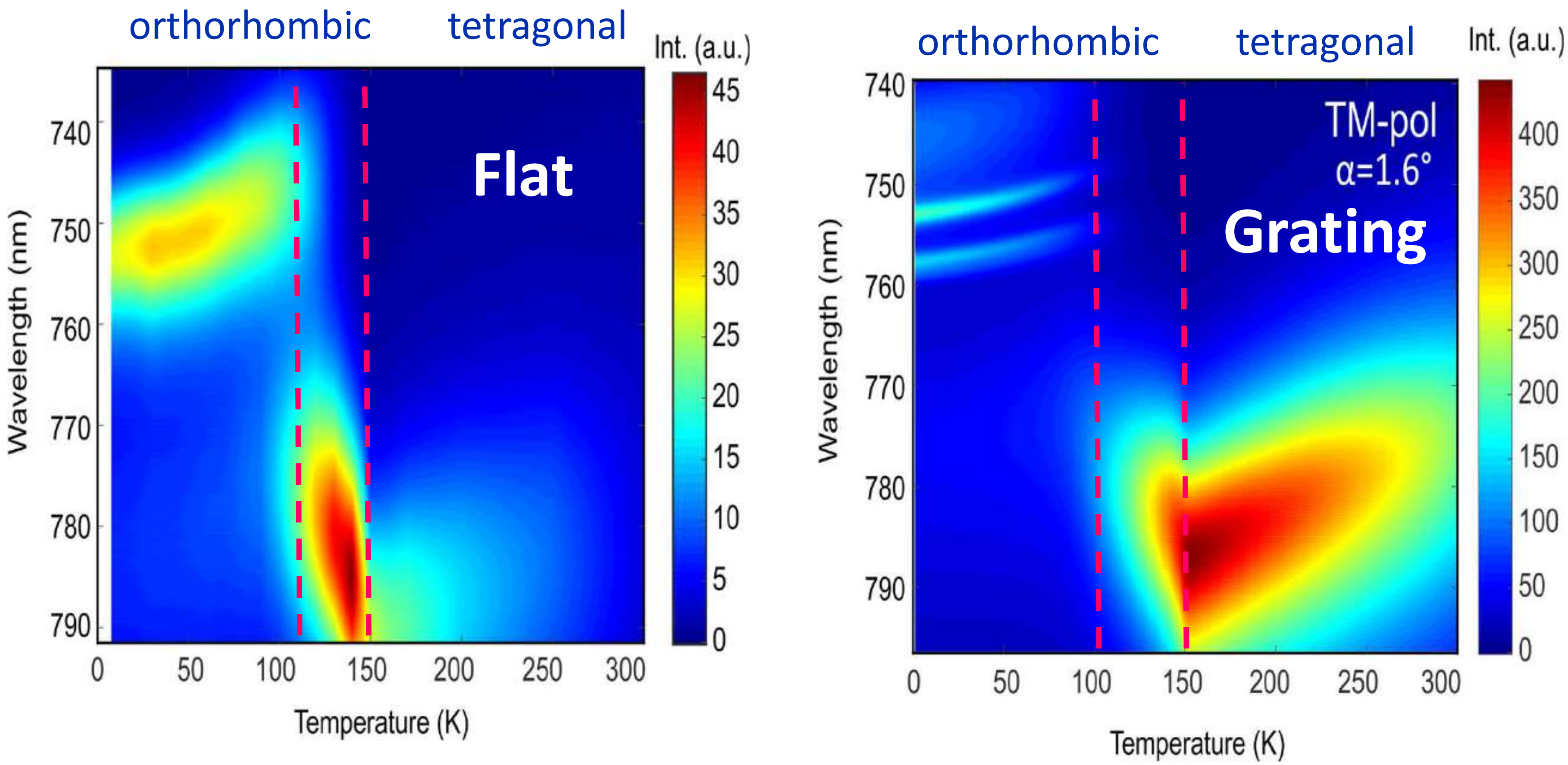

Tiguntseva et al. Applied Surface Science 473, 419-424 (2019)

Thresholdless narrow lines

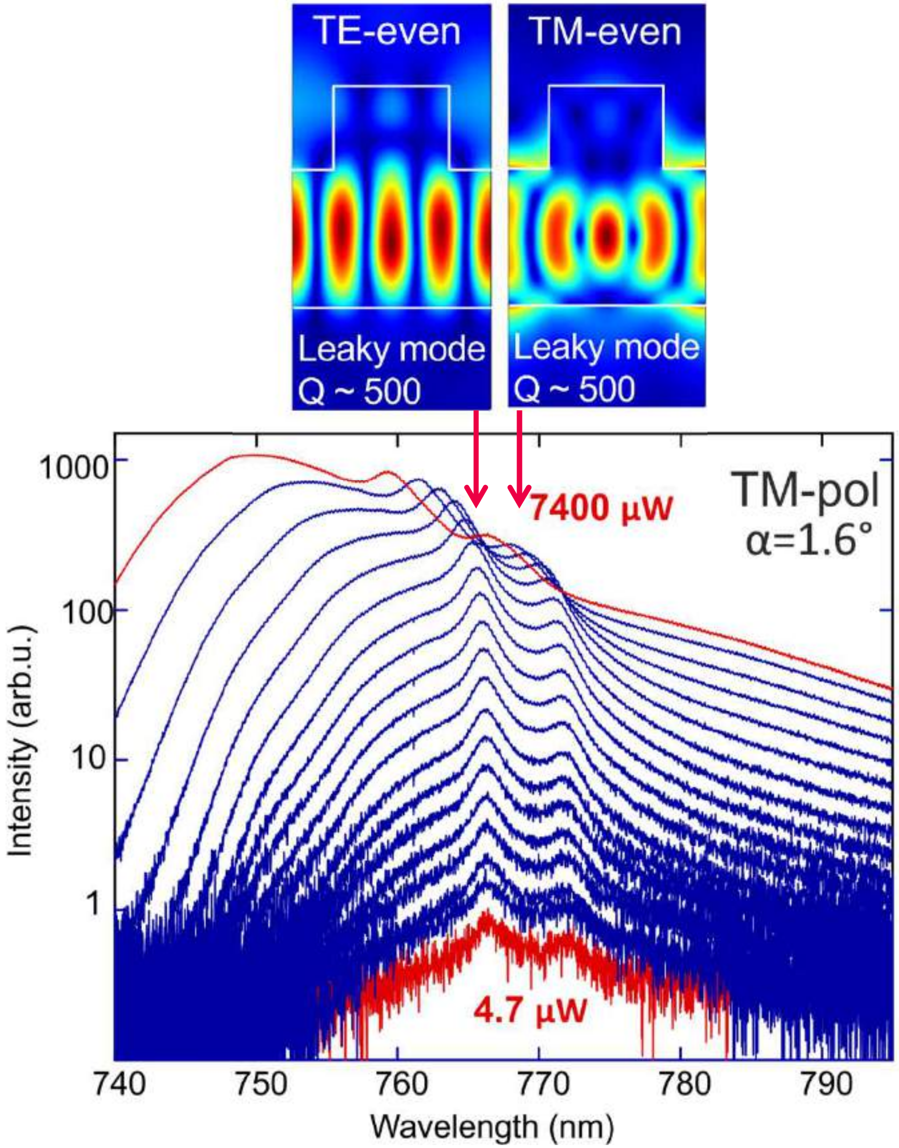

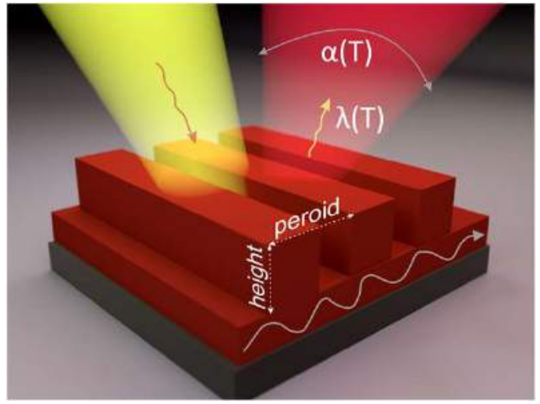

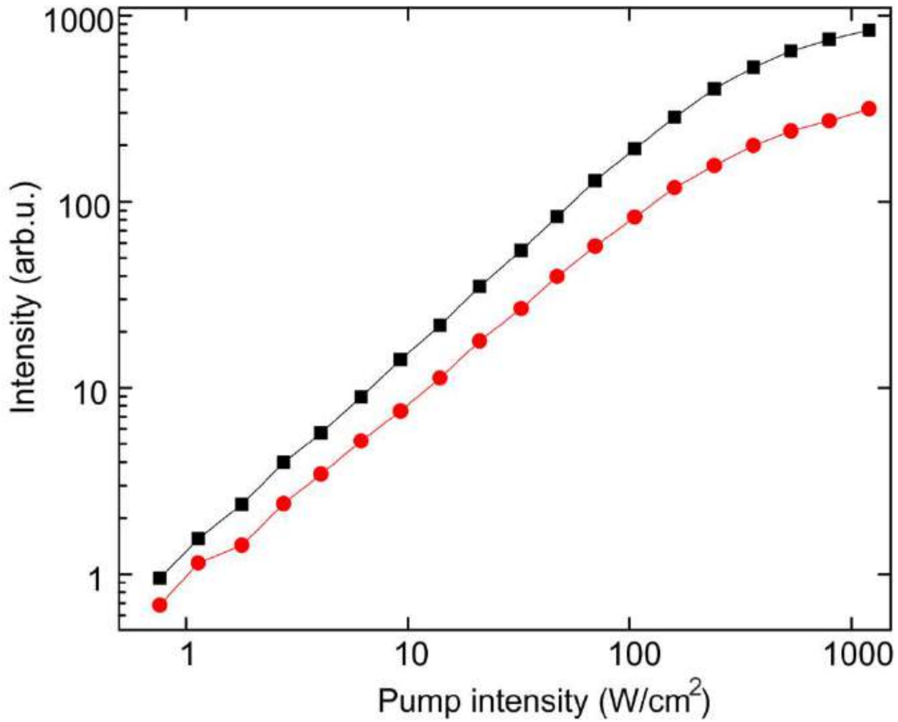

Tiguntseva et al. Applied Surface Science 473, 419-424 (2019)

nature photonics

LETTERS

https://doi.org/10.1038/s41566-017-0047-6

Continuous-wave lasing in an organic–inorganic lead halide perovskite semiconductor

Yufei Jia[1], Ross A. Kerner[2], Alex J. Grede[1], Barry P. Rand[2] and Noel C. Giebink[1*]

Hybrid organic–inorganic perovskites have emerged as promising gain media for tunable, solution-processed semiconductor lasers. However, continuous-wave operation has not been achieved so far[1–3]. Here, we demonstrate that optically pumped continuous-wave lasing can be sustained above threshold excitation intensities of ~17 kW cm^{-2} for over an hour in methylammonium lead iodide ($MAPbI_3$) distributed feedback lasers that are maintained below the $MAPbI_3$ tetragonal-to-orthorhombic phase transition temperature of $T \approx 160$ K. In contrast with the lasing death phenomenon that occurs for pure tetragonal-phase $MAPbI_3$ at $T > 160$ K (ref. [4]), we find that continuous-wave gain becomes possible at $T \approx 100$ K from tetragonal-phase inclusions that are photogenerated by the pump within the normally existing larger-bandgap

tetragonal phase inclusions may act as charge carrier sinks within the larger-bandgap orthorhombic phase host matrix, enhancing population inversion in a fashion analogous to host–guest organic–semiconductor gain media and inorganic quantum wells[13,14]. These results suggest a general strategy to design perovskite gain media for c.w. lasing and represent a key step towards the ultimate goal of a perovskite laser diode.

Figure 1 explores the amplified spontaneous emission (ASE) gain dynamics of a 120-nm-thick $MAPbI_3$ film deposited on a sapphire substrate using an InGaN pump diode ($\lambda_p = 445$ nm, intensity $I_p = 37.5$ kW cm^{-2}, 920-ns-long pulses at 100 Hz repetition rate) and a streak camera. In Fig. 1a, at a substrate temperature of $T = 169$ K, tetragonal-phase ASE is observed immediately following pump turn on, but ceases within ~100 ns, giving way to incoher-

Perovskite solar cells with Si nanoparticles

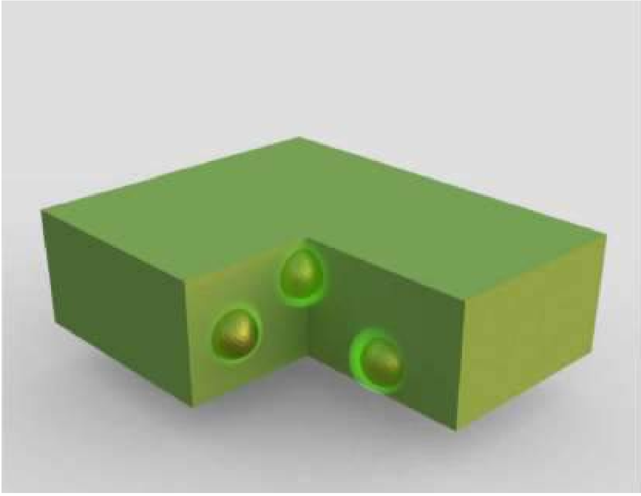

Plasmonics for improved photovoltaic devices

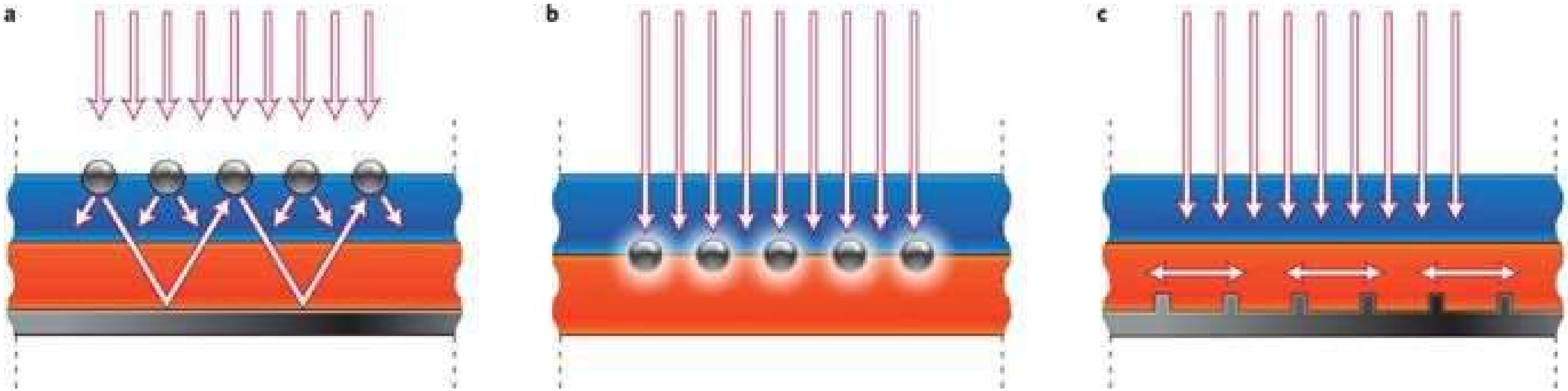

scattering

near-filed enhancement

waveguiding

Atwater and Polman, «Plasmonics for improved photovoltaic devices» Nature Materials volume 9, pages 205–213 (2010)

Silicon NPs vs Plasmonics for MAPI-PV

Resonant nanoparticles, shape (diameter)	Efficiency (%)/Fill factor (%)
Si, nanospheres, (100-200 nm)	**18.8/79**
Au@TiO_2, nanospheres (80nm)	18.2/75.5
Au@SiO_2, nanospheres (14 nm)	17.6/78.2
Au@SiO_2, nanorods (15×37 nm)	17.6/77.3
Au@TiO_2, nanorods (5×40) nm	16.8/74.7
Au, nanospheres (40 nm)	16.2/76
Au, nanospheres (40 nm)	16.1/68
Au@TiO_2, nanospheres (60 nm)	14.9/70
Au@SiO_2, nanospheres (45 nm) / nanorods (8×55 nm)	13.7/68
Ag@TiO_2, nanospheres (40 nm)	13.7/67
Au, nanostars (30 nm)	13.7/72.1 (regular) 8.7/71.2 (invert)
Au@SiO_2, nanospheres (100 nm)	11.4/64

Silicon NPs for pero-PV

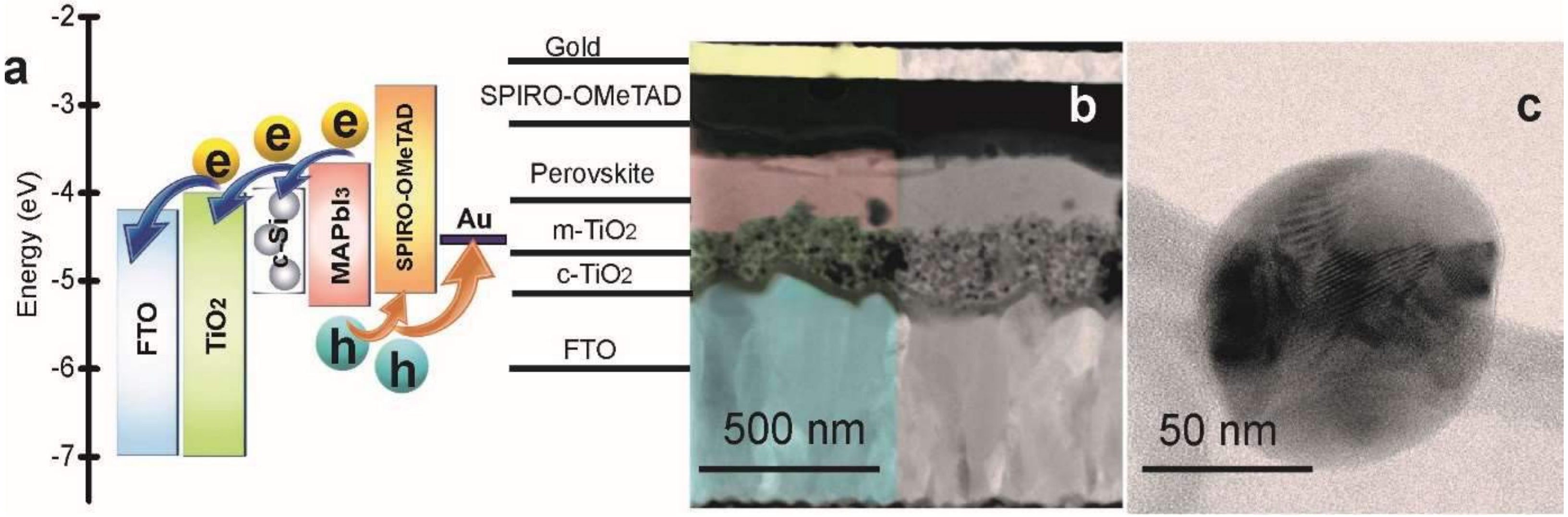

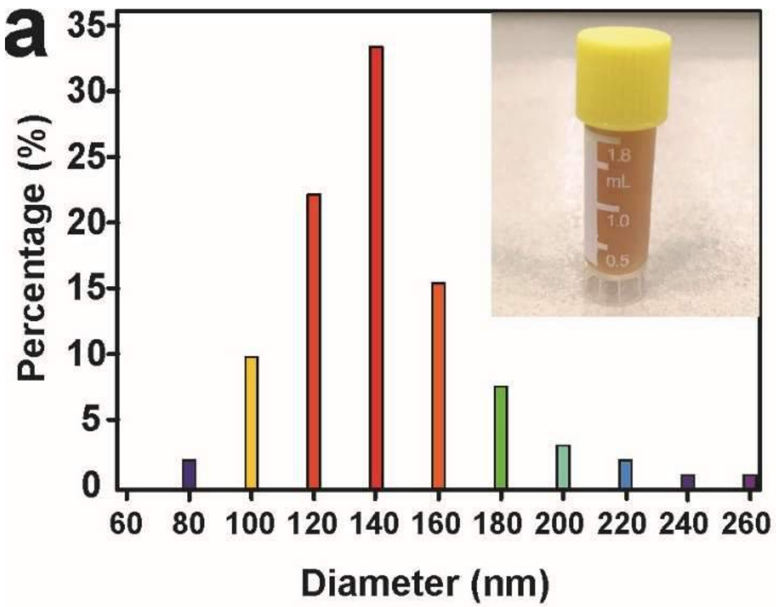

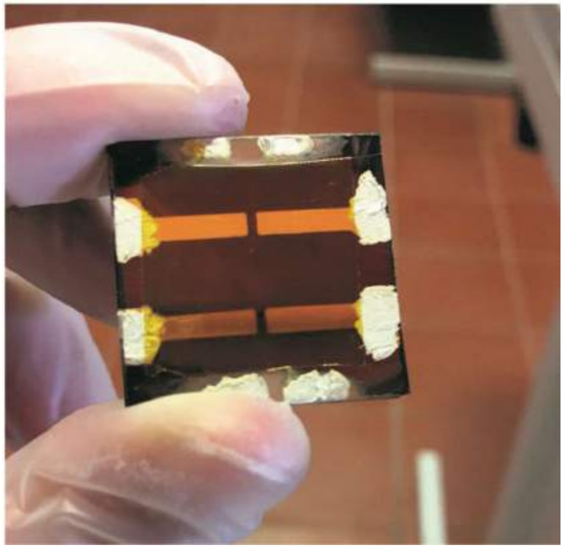

Furasova et al. Advanced Optical Materials, 1800576 (2018)

Silicon NPs for pero-PV

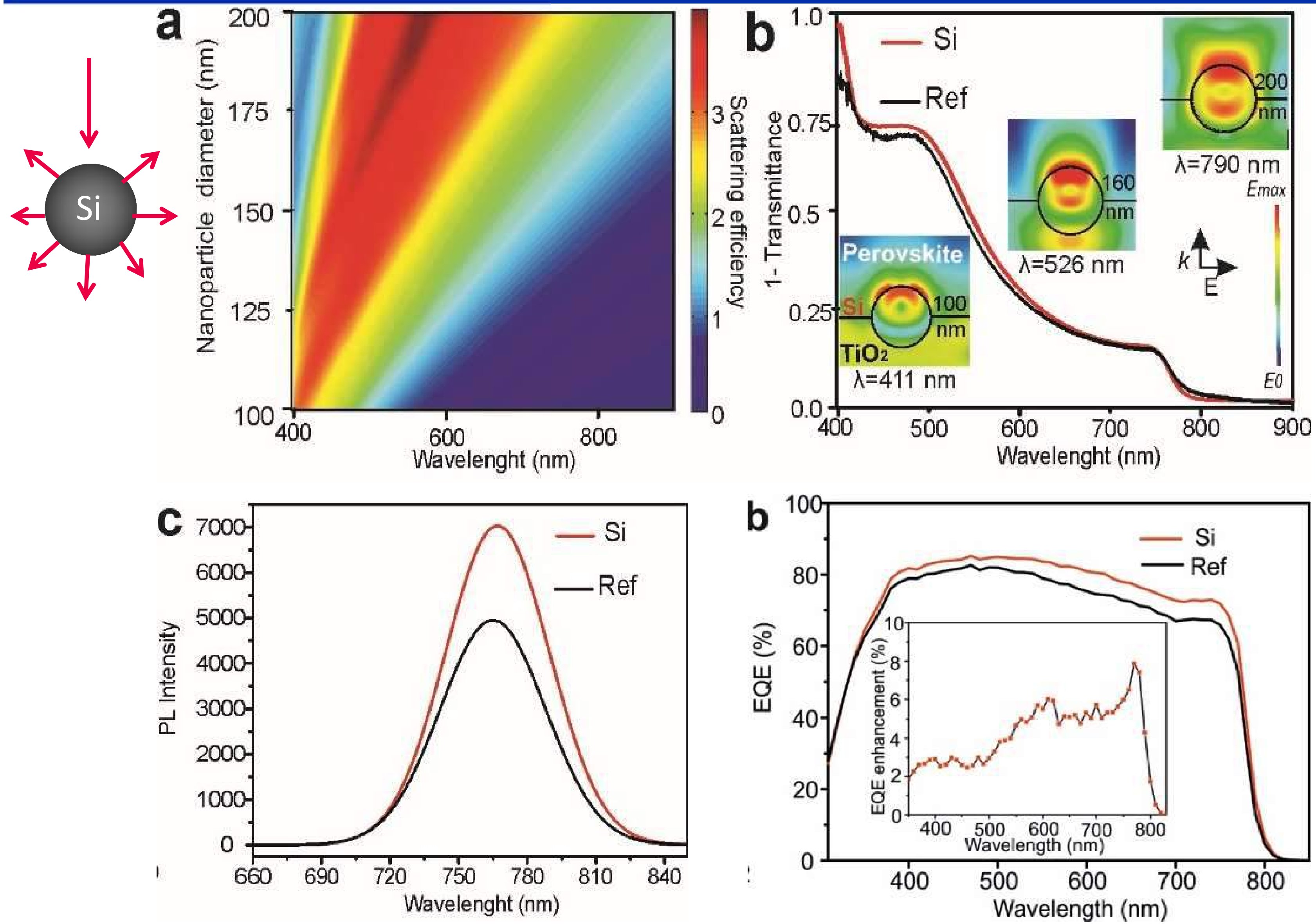

Furasova et al. Advanced Optical Materials, 1800576 (2018)

Silicon NPs for pero-PV

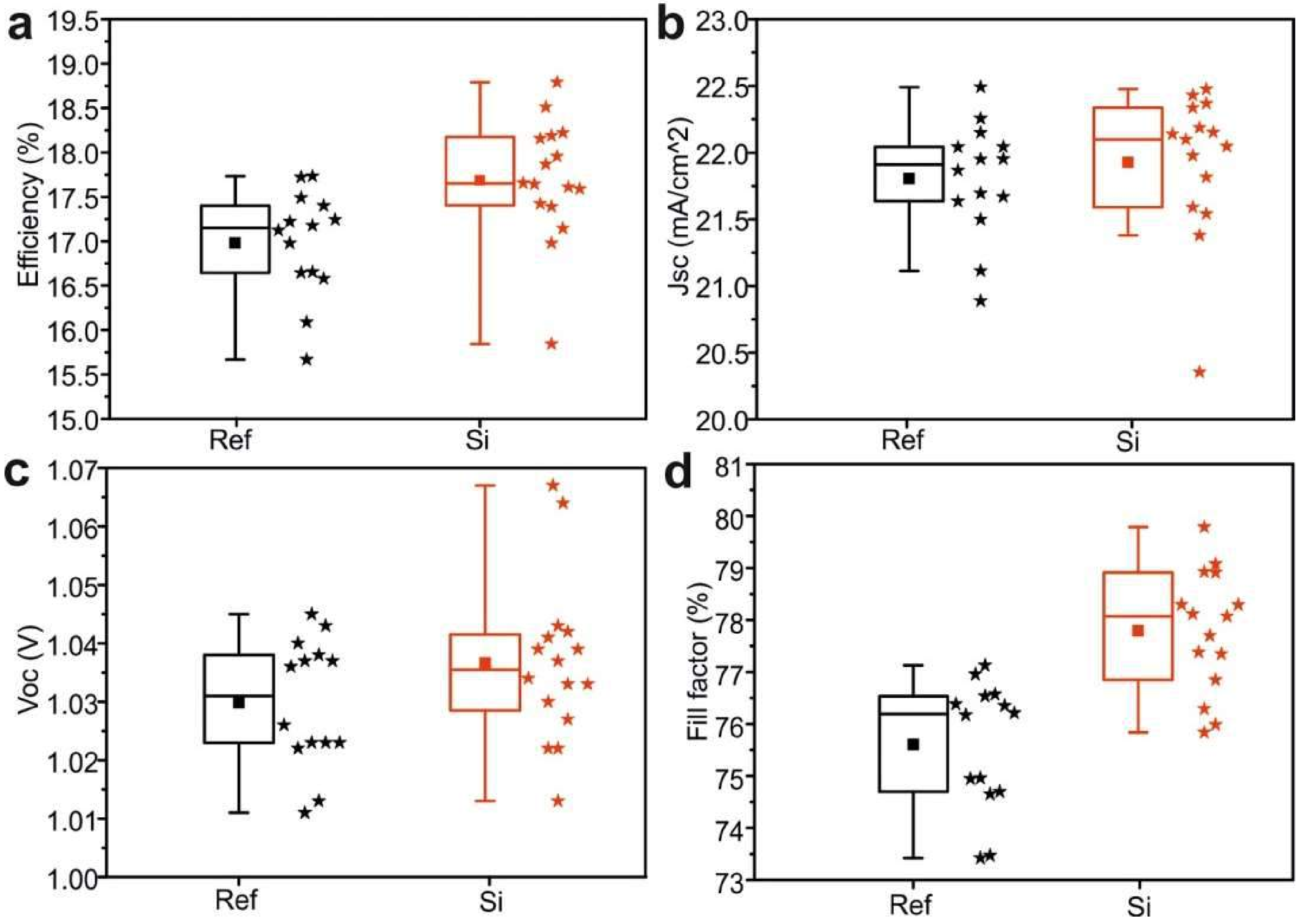

Furasova et al. Advanced Optical Materials, 1800576 (2018)